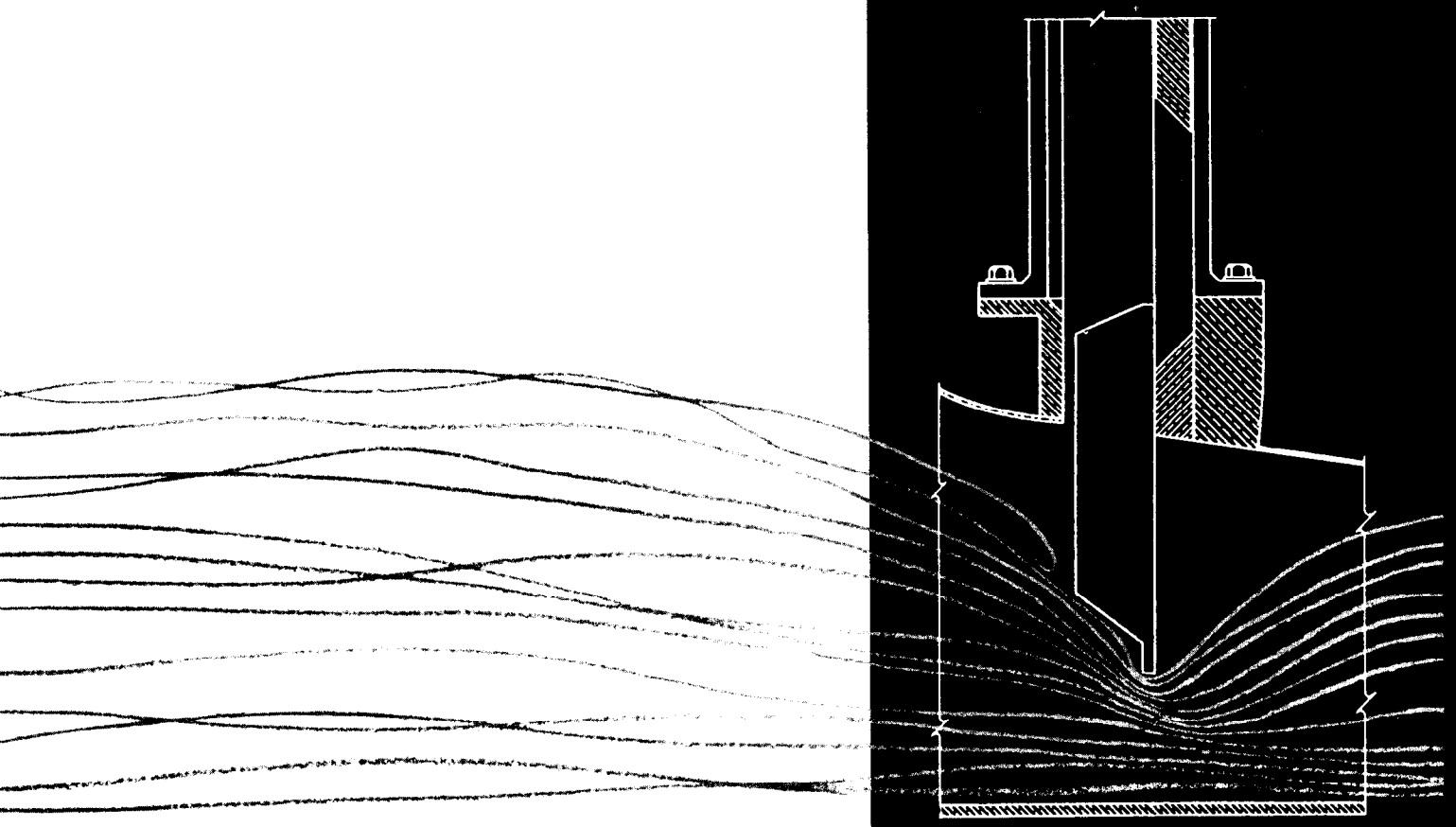

Hydraulic Downpull Forces on Large Gates

A Water Resources Technical Publication

RESEARCH REPORT NO. 4

United States Department of the

INTERIOR

Bureau of Reclamation

A WATER RESOURCES TECHNICAL PUBLICATION

Research Report No. 4

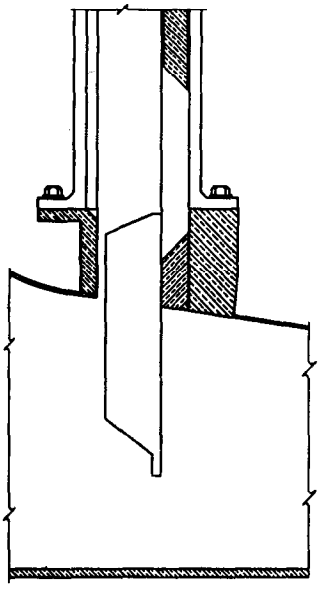

Hydraulic Downpull Forces on Large Gates

by R. I. Murray and W. P. Simmons, Jr.

Hydraulics Branch
Division of Research
Office of Chief Engineer

UNITED STATES DEPARTMENT OF THE INTERIOR

BUREAU OF RECLAMATION

In its assigned function as the Nation's principal natural resource agency, the Department of the Interior bears a special obligation to assure that our expendable resources are conserved, that renewable resources are managed to produce optimum yields, and that all resources contribute their full measure to the progress, prosperity, and security of America, now and in the future.

First Printing: 1966

U.S. GOVERNMENT PRINTING OFFICE
WASHINGTON : 1966

For sale by the Superintendent of Documents, U.S. Government Printing Office, Washington DC 20402, or the Water and Power Resources Service, Attn: D-922, PO Box 25007, Denver Federal Center, Denver CO 80225.

PREFACE

Research studies on a 1 : 35-scale laboratory model at the Denver Engineering Center provided hydraulic downpull parameters for designing outlet works emergency gates at the San Luis Dam, Central Valley Project, Calif.

Hydraulic downpull on downstream-seal, roller-mounted gates in entrance transitions of large conduits is primarily of concern to gate-hoisting equipment designers. The parameters obtained for the 17.50- by 22.89-foot San Luis gates can be adapted to the design of geometrically similar installations.

Application of the methods presented in Research Report No. 4, Hydraulic Downpull Forces on Large Gates, is illustrated by a typical problem example at the end of the text with a solution obtained through use of the proper design chart.

As most of the calculations for the reduction of raw data to downpull forces were made by digital computer methods, the description of the program, including its flow diagram of symbol definitions, and a printout sample are given.

Hydraulic Downpull Forces on Large Gates was written, and the material compiled, by R. I. Murray and W. P. Simmons, Jr., Hydraulics Branch, assisted by T. J. Isbester, who designed the test equipment and performed part of the test program. This research test program was conducted jointly by the Mechanical Branch of the Division of Design and the Hydraulics Branch of the Division of Research, both in the Office of the Chief Engineer at Denver, Colo.

Research Report No. 4 is in the Bureau's Water Resources Technical group. Much of the material was originally contained in the Bureau's internal Report No. Hyd–530, issued in limited quantity by the Hydraulics Branch.

Included in this publication is an informative abstract and list of descriptors, or keywords, and "identifiers". The abstract was prepared as part of the Bureau of Reclamation's program of indexing and retrieving the literature of water resources development. The descriptors were selected from the *Thesaurus of Descriptors,* which is the Bureau's standard for listings of keywords.

CONTENTS

List of Figures

PURPOSE

General studies were made to determine design parameters for hydraulic downpull on downstream-seal, roller-mounted gates located in entrance transitions of large conduits. Data are presented in both dimensional and nondimensional form on the effects of gate leaf and gate shaft geometry and of air vent size. The data were used to obtain downpull values for the San Luis Dam 17.50- by 22.89-foot outlet works emergency gates.

INTRODUCTION

General Considerations

Downpull is produced by the reduction of pressures when a fluid flows under a gate. In the absence of any flow, a gate that is completely submerged is subject to hydrostatic pressure that produces a buoyant force. This static condition is characterized by a uniform value of the piezometric head. The nonuniform distribution of piezometric head that is observed under flow conditions is due solely to the reduction of pressure, and the component of the force in the direction of gate travel computed from this pressure distribution is defined as downpull. It is taken as positive in the direction of gate closure.

Downpull is primarily of concern to the designer of gate-hoisting equipment. He must take into account the weight of the gate, the buoyant force, friction forces, and downpull. Downpull may be many times greater than the weight of a gate, and under some conditions it may become negative, indicating an uplift. This latter condition was observed during the course of this investigation.

A long-range program has been undertaken by the Bureau of Reclamation to establish general downpull design guidelines for a variety of gate designs, and for the three principal types of gate installations. The gates include upstream and downstream seal designs, roller train and fixed-wheel designs, and various bottom shapes. The types of gate installations consist of locations on the face of the dam over the conduit entrances, within the entrance transitions, and within or at the downstream end of the conduits.

Scope of the Present Investigations

This present study was part of the above long-range program and the objectives were fourfold:

1. To determine the downpull characteristics of a downstream-seal, roller-mounted gate located in the entrance transition of a conduit, and discharging under controlled conditions simulating maximum power generation at the powerplant and under "free discharge" conditions simulating a rupture in the tunnel.

2. To generalize the results into a form that would be applicable to future designs of a similar character. To this end the effect of lip extensions, seal size, gate thickness, and rounding of the upstream edge of the gate bottom were to be investigated. In addition the influence of holes in the bottom beam of the gate, the shape of the tunnel entrance, and the presence of a trashrack were to be determined.

3. To correlate the results of this investigation with the results of previous downpull studies.

4. To compare the pressure-computation method of determining downpull with the weighing method.

Objective 1 has been achieved, and objectives 2 and 3 are partially completed. Additional studies

are necessary for their completion. Objective 4 awaits studies to be made by the direct-weighing method.

Dimensional Analysis

The variables and parameters to be considered are given in the following list. The geometric parameters are shown in figure 1.

- P downpull force
- V velocity in the contracted jet issuing from beneath the gate
- ρ density
- μ viscosity dynamic
- g gravitational acceleration
- d gate thickness
- B gate width
- b tunnel width
- y_o tunnel height
- y gate opening
- e length of lip extension
- s length of seal extension
- a depth of recess in the gate well
- c width of gate slots
- r radius of the rounding on the upstream edge of the gate bottom
- α inclination of the bottom plate

From the principles of dimensional analysis, it is known that the functional relationship among these 16 variables can be expressed as a function of 13 dimensionless groups. With the gate thickness as the characteristic linear dimension the following functional relationship can be established:

$$\frac{P}{d^2\rho V^2}=F\left(\frac{y}{d},\frac{e}{d},\frac{s}{d},\frac{r}{d},\frac{a}{d},\frac{c}{d},\frac{y_0}{d},\frac{B}{d},\frac{b}{d},\alpha,\frac{Vd\rho}{\mu},\frac{V^2}{dg}\right). \quad (1)$$

Introduction of the plan area of the gate body ($A=Bd$) and manipulation of some of the variables produces an equivalent functional form with more meaningful variables.

$$\frac{2P}{\rho AV^2}=F\left(\frac{y}{yo},\frac{e}{d},\frac{s}{d},\frac{r}{d},\frac{a}{d},\frac{c}{d},\frac{y_0}{d},\frac{y_0}{B},\frac{d}{B},\alpha,\frac{Vd\rho}{\mu},\frac{V^2}{dg}\right). \quad (2)$$

The last of the dimensionsless variables will be recognized as a Froude number. It has significance only for free discharge because gravitational forces, which it characterizes, enter only into problems of free surface flow. For high headgates the gravitational effect on the free discharge flow pattern is negligible. Its effect on downpull is, therefore, negligible too; and since this investigation is limited to high headgates, the Froude number can be eliminated.

The dimensionless variable $Vd\rho/\mu$ is a Reynolds number. Its value for the prototype is so large that it ceases to be a significant variable, but models are generally operated at much lower Reynolds numbers than the prototype, and care must be taken to insure that this does not have a significant effect.

In this investigation a potential source of difficulty with Reynolds number arises when the upstream edge of the gate bottom is rounded. If the flow separates from this surface, the point of separation depends on Reynolds number; thus, the flow pattern and pressure distribution become dependent on Reynolds number. In the first phase of this investigation Reynolds numbers as low as 2×10^4 were encountered, but for reasons that are presented in the following section, this did not create any problem. In subsequent phases of the general study it will be a problem.

The effect of the parameters a/d, c/d, y_o/d, y_o/B, b/B, and α lie outside the scope of the proposed investigation. The values that were used are given below:

$a/d=0.564$	$y_o/B=1.308$
$c/d=1.306$	$b/B=0.759$
$y_o/d=5.353$	$\alpha=0.$

The functional relationship to be determined in the proposed investigation now reduces to:

$$\frac{2P}{A\rho V^2}=\mathsf{K}\left(\frac{y}{yo},\frac{e}{d},\frac{s}{d},\frac{r}{d},\frac{Vd\rho}{\mu}\right). \quad (3)$$

The dependent variable will be called the downpull coefficient and will be denoted by K. Thus

$$\mathsf{K}=\frac{2P}{A\rho V^2}. \quad (4)$$

Scope of Tests and Report

In the tests reported herein, s/d and r/d were held at the constant values of 0.15 and zero, respectively. With a sharp corner on the upstream edge of the gate there is no question but that the flow separates at this corner (fig. 1). The second point of separation, if one occurs, depends upon gate opening and length of lip extension. With the point of separation fixed at the upstream bottom corner of the leaf under test, and since boundary shear is assumed to be negligible, the Reynolds num-

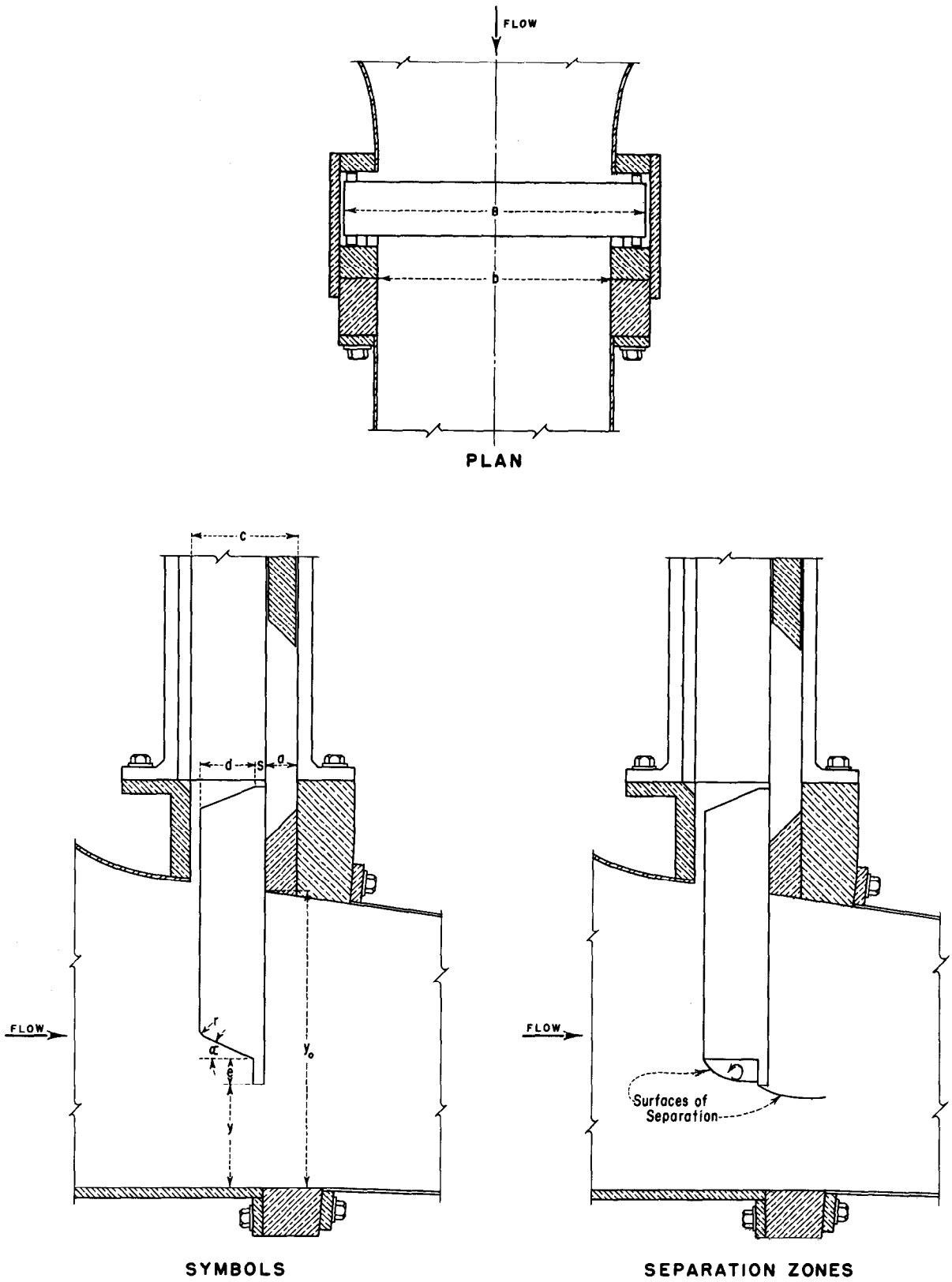

FIGURE 1.—Definition sketches.

ber is eliminated as a variable. The functional relationship for the first phase of the investigation is therefore represented by

$$K = K(y/yo, e/d). \quad (5)$$

Four values of the parameter, e/d, were investigated: 0.2, 0.4, 0.6, and 0.8. Each value was tested at three flow conditions: Controlled discharge representing maximum power generation, free discharge of the gate, and free discharge 4 tunnel diameters downstream from the transition section to represent a ruptured tunnel.

In addition to curves showing the downpull coefficient, curves giving the computed prototype downpull forces and the flow rates are presented. A few selected pressure distributions on the model are also given.

CONCLUSIONS

1. Dimensionless downpull coefficient data are presented and may be used with confidence on gate structures of similar geometric design.

2. The test data are in reasonable agreement with results of other investigators considering differences in the geometries studied.

3. Uplift forces severe enough to prevent closure of the gates under their own weight can act on the gates unless provisions are made to prevent or reduce the uplift (fig. 2).

4. The proximity of the downstream wall of the gate shaft and the top and bottom seals of the gate leaf have great effect upon downpull and uplift forces. With proper shaping of this wall by recesses and offsets the forces can be significantly reduced (figs. 3 and 4).

5. The ratio of gate lip extension to leaf thickness greatly affects downpull and uplift (fig. 4). Increases in lip extension reduce both downpull and uplift. A lip extension ratio of 0.55 was selected as the best compromise between structural and hydraulic considerations.

6. The lip extension ratio of 0.55, and the revised offsets on the downstream wall of the well, produce reasonable downpull forces and sufficiently low uplift forces so the gates will operate satisfactorily.

7. Three-dimensional effects, i.e., the effects of gate slots and sidewalls, significantly influence the pressures on the underside of the gate leaves.

8. A maximum downpull force of about 710,000 pounds (710 kips) will occur during emergency closures of the San Luis gates if free discharge conditions occur at the downstream gate frame.

9. A downpull force of about 800 kips will occur if a catastrophic rupture occurs in the penstocks some distance downstream from the San Luis gates. This force is greater than for free discharge conditions because subatmospheric pressures would exist under the top seal.

10. A downpull force of about 405 kips will occur on the San Luis gates if the closure is made while maximum power generating flows of 4,225 c.f.s. are passing through the turbines.

11. A minimum of 4,230 c.f.s. of free air must be admitted to the conduit just downstream from each San Luis gate to maintain an ambient pressure not lower than one-half atmosphere subatomospheric during closures with severely ruptured penstocks.

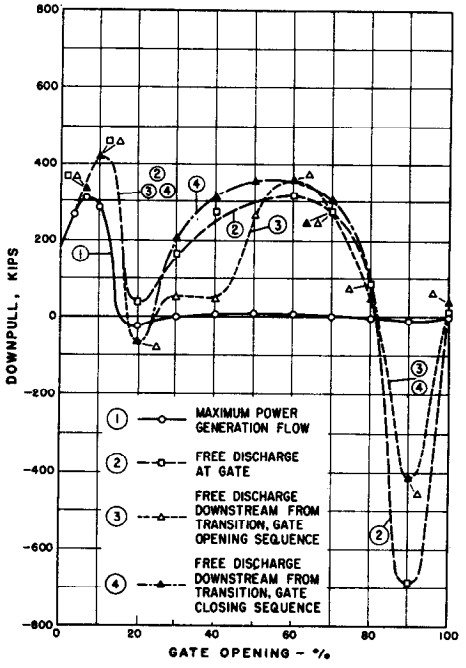

A. EFFECT OF VARIOUS OPERATING CONDITIONS - $\%_d = 0.8$

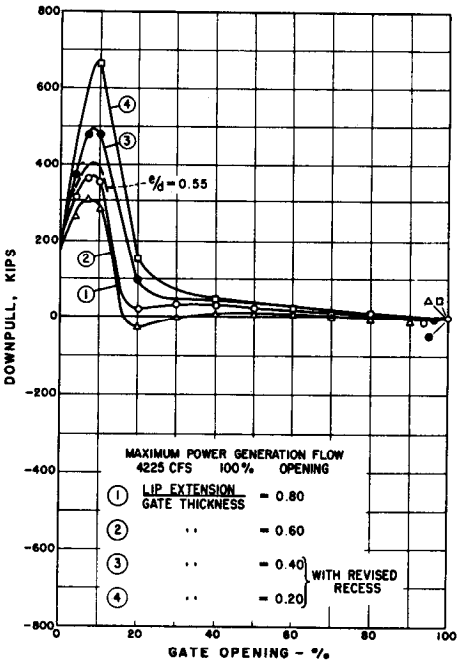

B. EFFECT OF LIP EXTENSION- MAXIMUM POWER GENERATION FLOW
Q = 4 230 C.F.S.

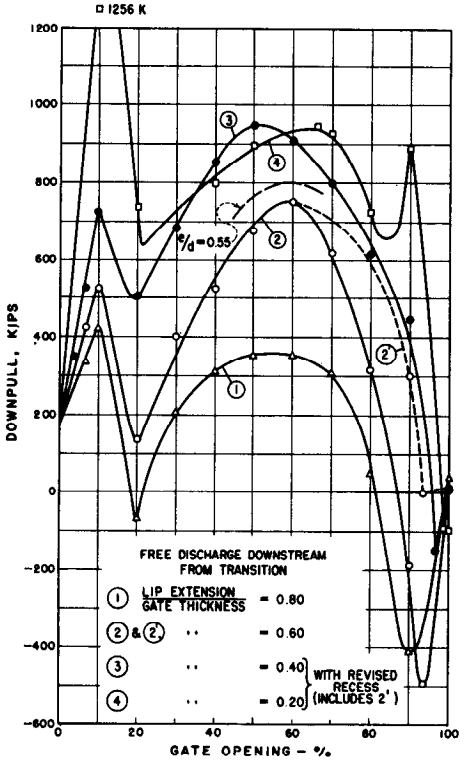

C. EFFECT OF LIP EXTENSION- FREE DISCHARGE DOWNSTREAM FROM TRANSITION
Q = 30 000 C.F.S.

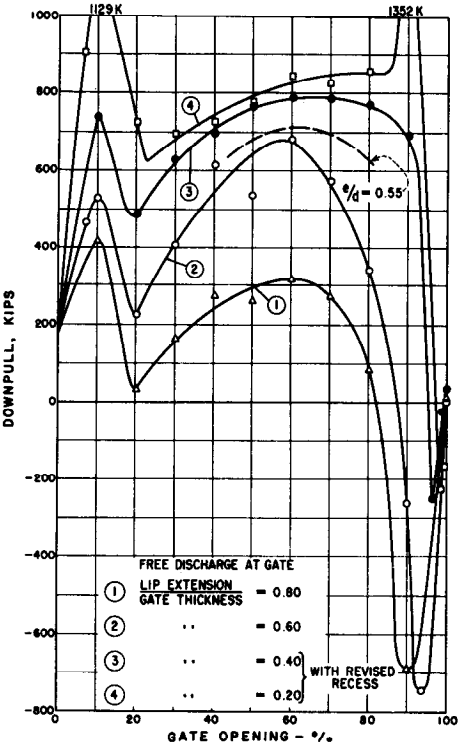

D. EFFECT OF LIP EXTENSION- FREE DISCHARGE AT GATE
Q = 45 000 C.F.S.

$\frac{\text{Seal Extension}}{\text{Gate Thickness}} = 0.15$

FIGURE 2.—Prototype downpull forces.

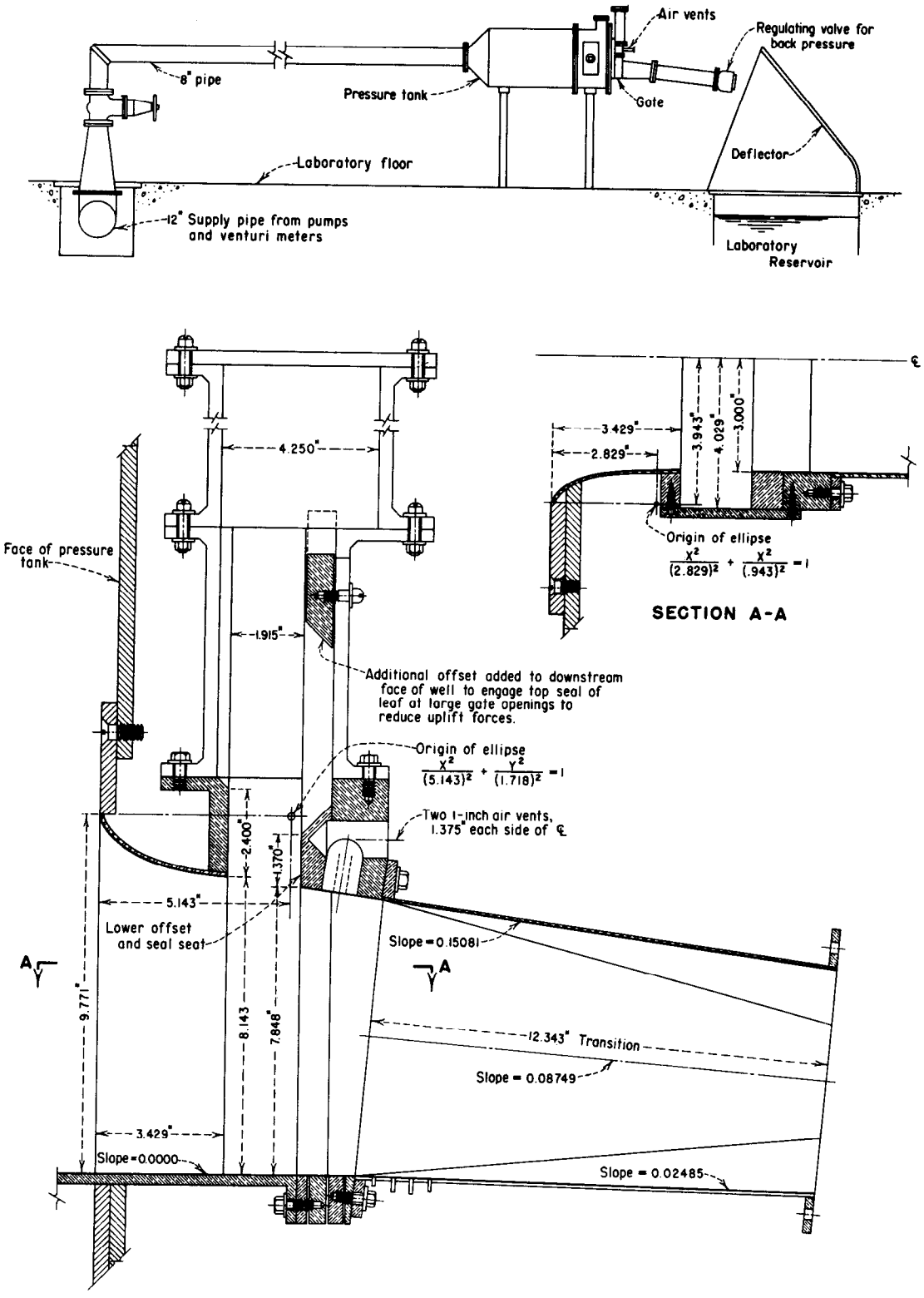

FIGURE 3.—Test facilities and 1:35 model of San Luis gate.

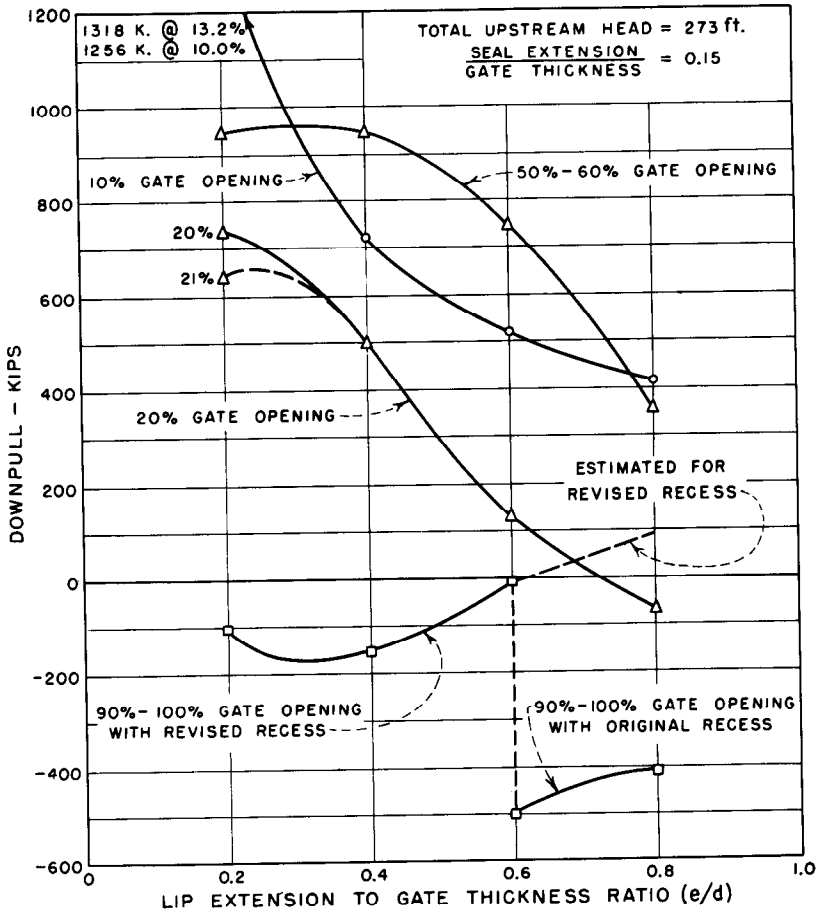

A. EFFECT OF LIP EXTENSION ON DOWNPULL

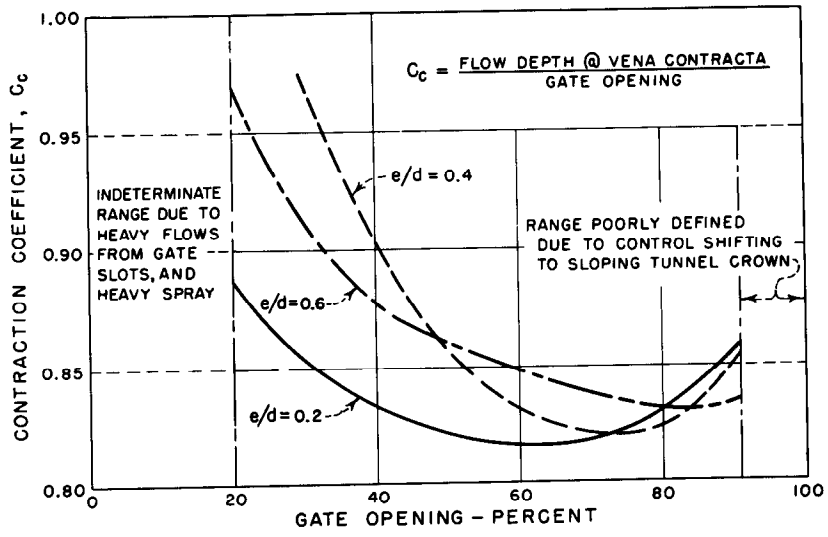

B. CONTRACTION COEFFICIENTS

FIGURE 4.—Effect of lip extension on downpull and contraction coefficients.

THE MODEL

The gate used for the investigation was a 1:35-scale model of one of the four closure gates in the outlet works of San Luis Dam in the Central Valley Project (figs. 5 and 6). The gate leaves have downstream seals and downstream skinplates. They are roller mounted in a gate well near the bellmouth entrance of the tunnels that lead to the powerplant at the base of the dam. At the gate well the tunnel has a rectangular cross section that is approximately 23 feet high and 17.5 feet wide. Just downstream from this section there is a transition to a 17.5-foot-diameter circular tunnel. The maximum water surface elevation in the reservoir is 273 feet above the invert of the tunnel at the gate section.

Test Apparatus

The test apparatus is shown in figures 3, 7, and 8. A 3-foot-diameter pressure tank with flow distributing baffles at the upstream end represented the reservoir. The 1:35 scale intake structure of the San Luis outlet works was mounted on a bulkhead at the end of the tank. The model was built from galvanized sheet metal, brass plate, and bar stock. The bottom portion of the leaf was made removable so that lip extensions of $0.2d$, $0.4d$, $0.6d$, and $0.8d$ could be tested.

To maintain the same overall height of the gate leaf for different lip extensions, the model leaf was made in two parts and bolted together (figs. 7 and 8). This made it possible to insert shims between the two parts to compensate for different lip extensions. This construction, especially when shims were inserted, interrupted the equal spacing of the horizontal beams. The effect which this may have had on the results is discussed later in the report.

In certain details the model deviated from the San Luis gate. These deviations are as follows:

1. The top and side seals of the prototype were represented in the model by brass bars of rectangular cross section.
2. The bottom seal was modeled by a strip of sheet metal across the bottom of the skinplate.
3. The roller trains of the prototype were represented on the model by brass bars on the front and back surfaces, and by brass plates placed on edge across the bottom to form the gate roller extensions.
4. The roller extensions were omitted on the bottom of the leaf for the smallest lip extension.

In addition to the above model deviations from the San Luis gate, certain features of the model should be noted:

1. The model of the tunnel was terminated 4 diameters downstream from the transition section without incorporating the small horizontal bend (less than 10°) of the prototype.
2. The air vents in the top of the downstream gate frame were originally modeled to the equivalent size of the proposed 12-inch vents. Later they were revised and considerably enlarged. However, the length of the air ducts was not modeled. Instead, valves located near the gate were used to control the airflow.
3. The trashrack and its foundation were omitted from the model.
4. The full height of the gate well was not modeled.

The implications of terminating the tunnel and not modeling the air ducts are discussed later in this report. The effect on downpull of omitting the trashrack is to be the subject of a later phase of the investigation, but it is believed that the effect is negligible.

The model of the gate well was terminated at a sufficient height above the gate to insure a negligible influence on downpull. This statement is supported by the uniformity of the pressures measured in the gate well. The pressure exerted by the cover plate of the model well is the same as would

be exerted in a taller open well by the higher column of water that would form.

The recess near the bottom of the downstream wall of the gate well was modeled to conform to the preliminary prototype design. After testing the first two lip extensions (e/d=0.8 and 0.6), the recess was revised to minimize the "uplift" that was discovered during the tests. This revision is discussed more fully later in the report.

Instrumentation

The model gate was instrumented with 27 piezometers: 18 on the bottom beam, 4 on the gate lip, 2 on the bottom of a roller extension, 2 at the top of the skinplate, and 1 on the top beam (fig. 7). In addition, 1 piezometer was located in the pressure tank, 1 was located at the top of the tunnel just downstream from the gate and midway between the two air vents, 7 were located on the centerline of the invert downstream from the gate, and 28 were located on the bellmouth entrance. After the first series of tests (e/d=0.8) three piezometers were installed in the walls of the gate well to indicate bonnet head.

The piezometers on the invert were intended to reveal the head and location of the vena contracta of the jet issuing from beneath the gate, but the expectation was not realized because of the influence of the transition section and of the secondary flows down the gate slots and down the backface of the leaf (skinplate) from the gate well.

The piezometer lines from the model were taken to a manometer board where the piezometric heads were indicated by water columns (fig. 9). The scale on the manometer board was expressed in feet and subdivided to hundredths of a foot. The reading of 0.79 corresponding to the elevation of the tunnel invert at the gate was determined with a surveyor's level. This was the datum used for all head measurements.

The manometer board was divided into four sections, each of which could be independently pressurized with air. The air pressure was measured by mercury U-tube manometers. This arrangement, while causing a small loss of accuracy, eliminated the need for a tall manometer board equipped with a ladder for taking readings.

The gate was raised and lowered by a threaded shaft that passed through the cover plate on the gate well. A series of spacer templates was used between the top of the cover plate and the screw handle to set the gate openings. All settings were made with the screw being turned to open the gate, and the templates provided approximately 10 percent increments of gate opening. For intermediate openings the distance from the top of a template to the bottom of the screw handle was measured.

After the first series of tests, it was deemed necessary to measure the depth of water in the free discharge jet. This was accomplished with a point gage. The measurement could not be made accurately because of the turbulent surface, but a satisfactory estimate was obtained for most gate openings.

Flow rate was measured with calibrated Venturi meters in the laboratory's main water-supply system.

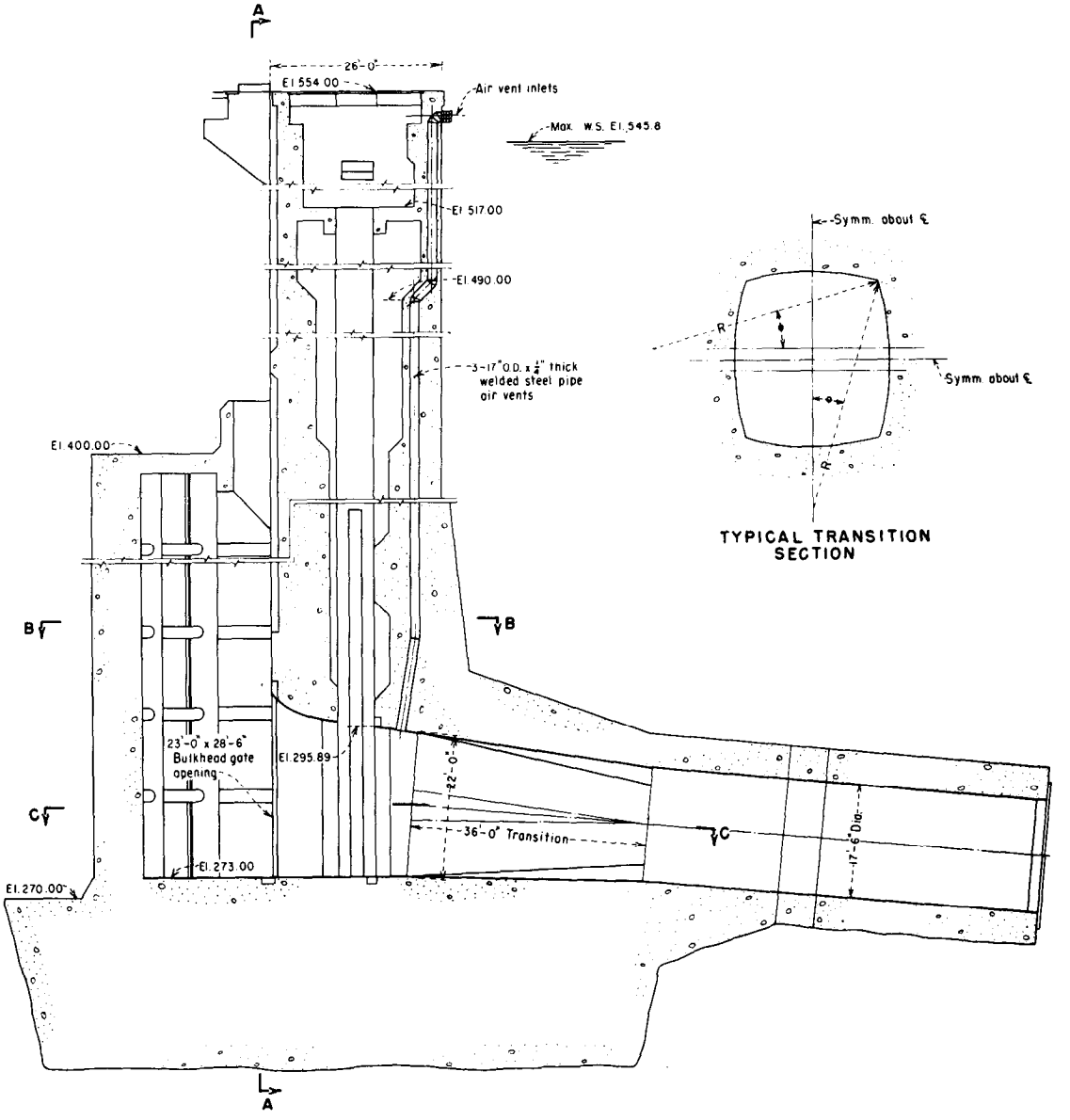

FIGURE 5.—Typical trashrack, gate structure, and conduit, San Luis Dam outlet works.

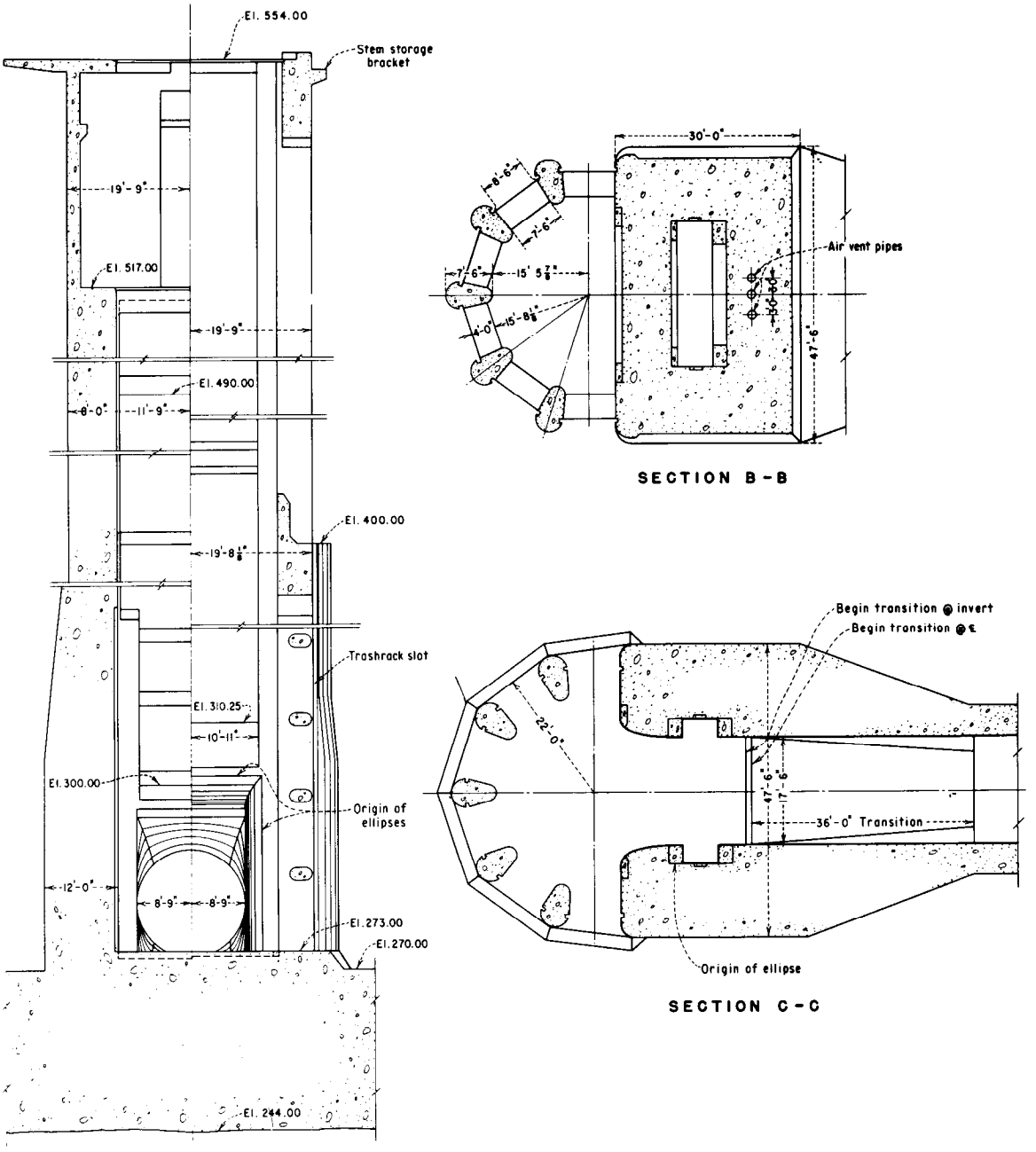

FIGURE 6.—Typical trashrack, gate structure, and conduit, San Luis Dam outlet works.

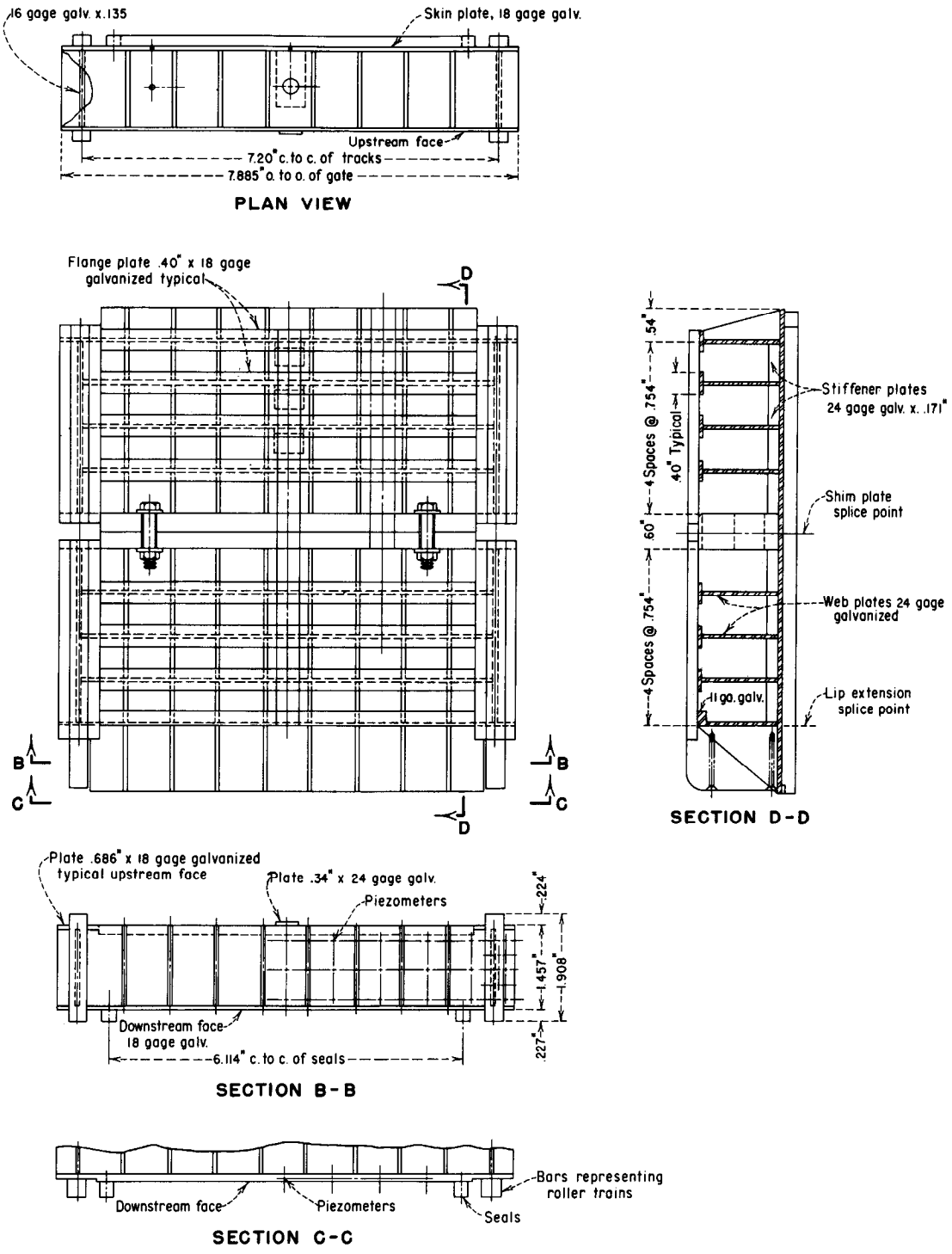

FIGURE 7.—Detail of model gate leaf.

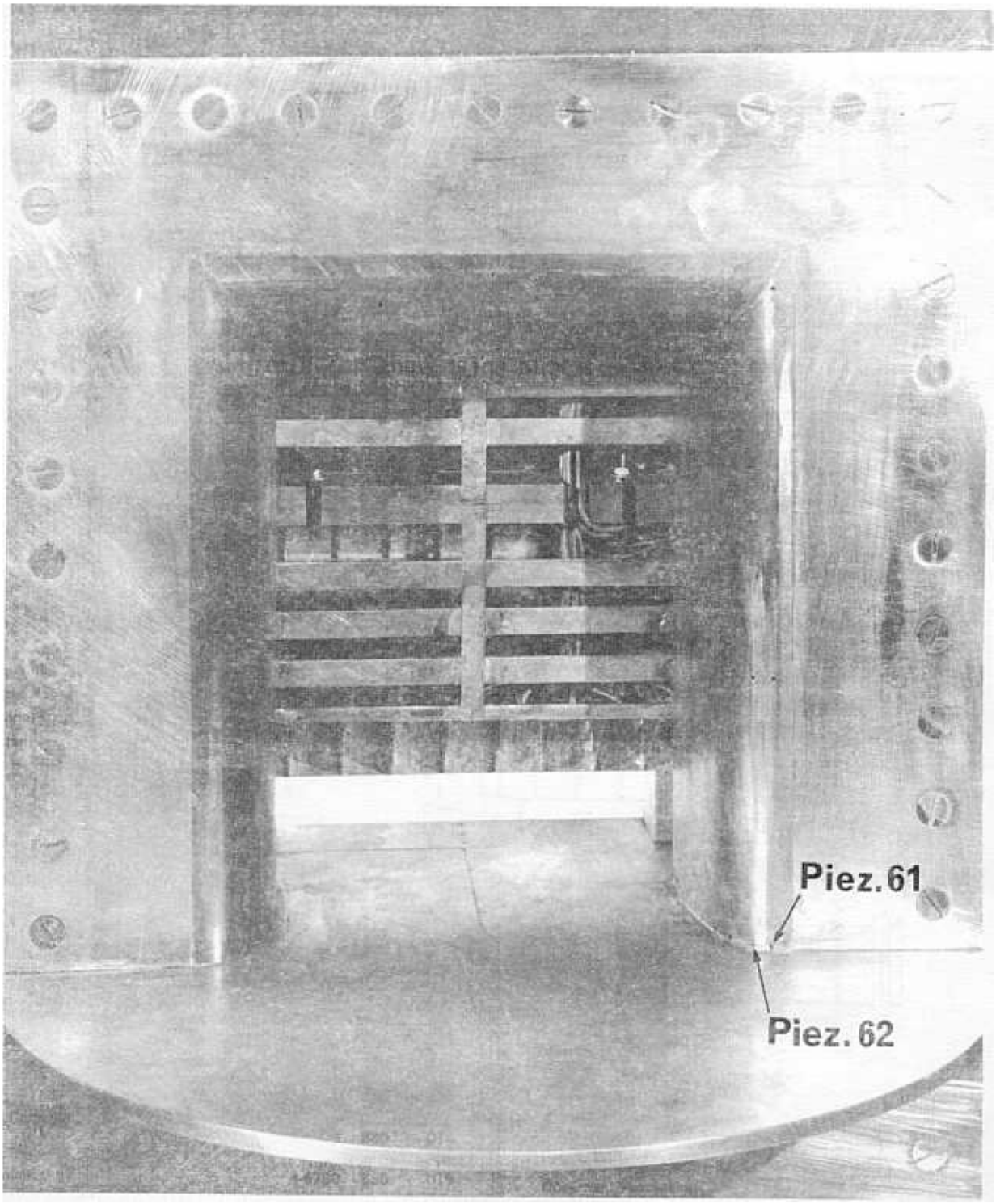

FIGURE 8.—Photograph of model gate.
View looking downstream into bellmouth entrance, showing open upstream face of gate leaf. Bottom extension is 0.8d.

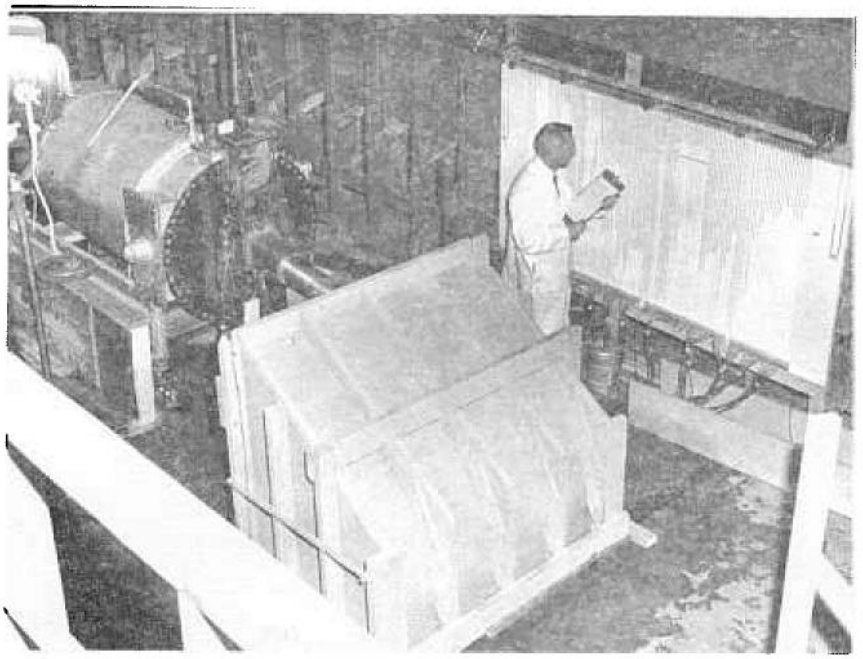

A. Overall view of pressure tank, gate structure, downstream piping, splash deflector, and manometer board.

B. Gate with downstream conduit removed.

C. Flow at 60 percent opening with transition and short downstream conduit in place.

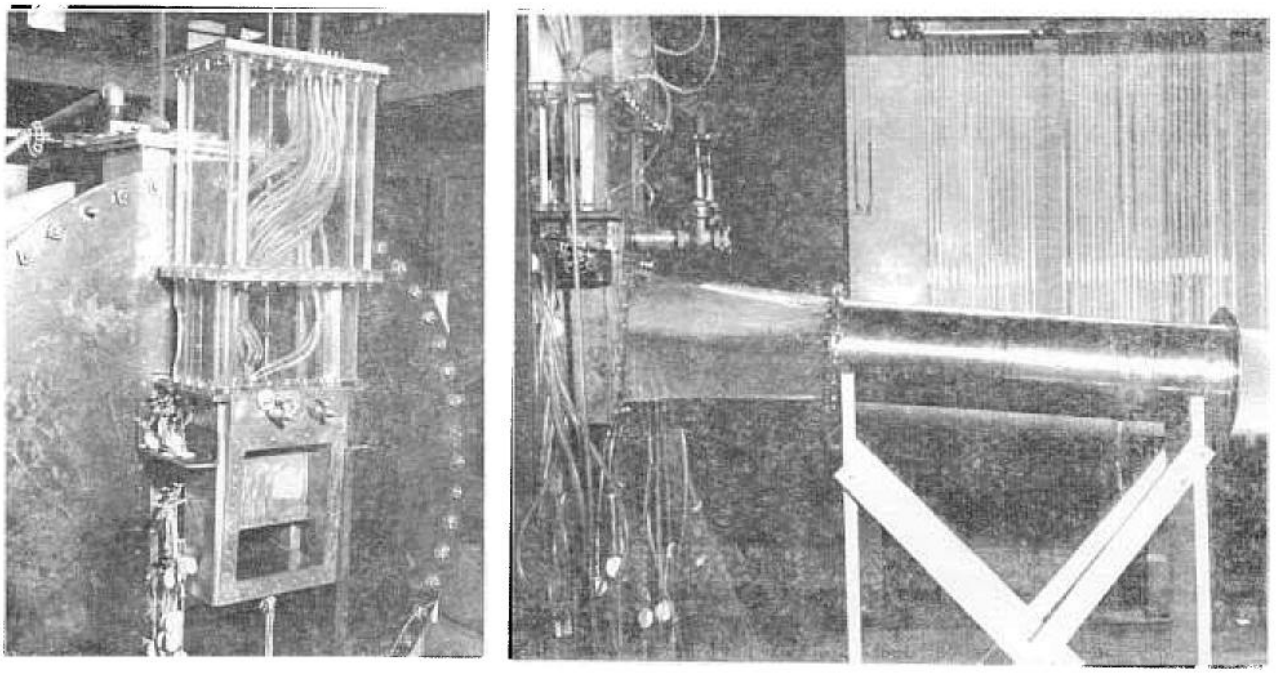

FIGURE 9.—Photographs of model gate.

INVESTIGATION

Experimental Procedure

For the condition of controlled discharge, representing maximum power generation at the powerplant, a hollow-jet valve was mounted at the end of the 4D-long model tunnel and adjusted to pass a flow of 0.583 c.f.s. with the model gate fully opened and with a head in the tank of 7.80 feet. These values were equivalent to 4,225 c.f.s. and a 273-foot head. To obtain these conditions the hollow-jet valve and a gate valve located upstream from the pressure tank had to be adjusted simultaneously. After the proper settings had been achieved, the hollow-jet valve was left without further adjustment, but the gate valve was adjusted for each gate opening of the model to maintain a tank head representing 273 feet. This valve could not be set precisely for every gate opening, so small discrepancies were adjusted by computation.

For free discharge downstream from the transition section, representing a catastrophic rupture in the penstock, the hollow-jet valve was removed and the proper tank head was maintained by adjusting the gate valve. For large gate openings the reduction of area through the transition section produced a back pressure at the gate. The gate was thus completely submerged and the flow pattern was dynamically similar to the flow pattern for controlled discharge.

As the gate was closed from the full open position, the contraction in the flow pattern caused a reduction in pressure downstream from the gate. For the first series of tests ($e/d=0.8$) the valves to the 12-inch-diameter (prototype) air vents were opened wide as soon as the pressure indicated by piezometer 28, located at the crown of the tunnel between the air vents, became atmospheric. With ventilation and fairly large gate openings, the flow pattern became similar to a free discharge flow pattern, with a hydraulic jump in the transition section.

When the gate was closed further, the prototype 12-inch air vents were not adequate to maintain a pressure close to atmospheric. In fact, even with the valves on the air vents removed, the pressure downstream from the gate dropped to a value equivalent to minus three atmospheres on the prototype—a physically impossible situation on the full-sized structures. Nevertheless, data were recorded, and the downpull was adjusted by computation to correct for this unrealistic condition. Later, the vents were enlarged to represent two 36-inch-diameter conduits.

With more closure of the gate, the hydraulic jump was swept out, the flow became ventilated from the downstream end of the tunnel, and the pressure downstream from the gate became nearly atmospheric.

As soon as the air vents were opened, it became impossible to maintain the line to piezometer 28 full of water. For measurements under these conditions the piezometer line was blown free of all water and connected to a U-tube manometer containing either water or mercury, depending on the magnitude of the negative pressure to be measured.

After the first series of tests, it was decided that the size of the air vents on the model should be increased so that enough air could be introduced to prevent the pressure in the model from dropping below the cavitation threshold of the prototype. This threshold was taken as -32.5 feet of water, which on the model would be -0.93 feet. The following procedure was adopted and used for all subsequent tests.

1. The air vents were closed whenever the equivalent prototype pressure indicated by piezometer 28 was greater than -32.5 feet of water.
2. When the equivalent pressure became less than -32.5 feet the air vents were opened just enough to maintain the threshold pressure.
3. After the flow became ventilated from the end of the tunnel, the air vents were closed.

The purpose of this procedure was to test the gate under the worst possible prototype conditions, namely, the pressure levels that would occur in the absence of any ventilation. When the air vents were opened, it was not to simulate the effect of air

vents in the prototype, but rather, to simulate the void or vapor filled region that would be produced by severe cavitation, and which would prevail at a pressure of about −32.5 feet of water at San Luis Dam.

A photograph of the model operating under simulated cavitation conditions is given in figure 9C. Undoubtedly the flow pattern would be somewhat different with real cavitation, but this was the best simulation that could be achieved in the model.

On closure cycles, the gate opening at which the cavitation threshold was reached was between 60 and 70 percent for lip extensions of 0.2, 0.4, 0.6, and 0.8d. Ventilation from the end of the 4D-long tunnel occurred between 30 and 40 percent gate openings with $e/d=0.8$ and 0.4, and between 40 and 50 percent openings for $e/d=0.6$. For $e/d=0.2$ and a gate opening of 30 percent, sufficient air to hold the cavitation threshold could not be introduced through the two 36-inch vents without having the flow ventilate from the downstream end of the tunnel.

However, when the air vents were closed, the tunnel again filled and the pressure fell below the cavitation threshold. No data were recorded for these conditions. At a 20-percent gate opening the flow was freely ventilated from the end of the tunnel.

For opening cycles with $e/d=0.8$ the flow ventilated from the downstream end of the tunnel until a gate opening in the 50- to 60-percent range was achieved. But because only the gate closure sequence seemed to have practical significance, tests of gate opening sequences were discontinued.

Free discharge at the gate was obtained by replacing the transition section and tunnel with an open channel. The pressure associated with piezometer 28 was taken as atmospheric for all gate openings even though small positive pressures were observed for gate openings close to 100 percent. These positive pressures were due to the sloping crown of the tunnel.

Readings of the water columns on the manometer board were recorded photographically. Because there was some fluctuation of the water columns, an attempt was made to take the pictures when the piezometric head in the tank was at its mean value.

It was soon observed, however, that the readings of the other piezometers were not always the same for a given tank piezometer reading. In fact, there was no detectable correlation at all. This was particularly true of the piezometers located on the bottom beam of the gate and on the roller extension. Readings of the piezometers located near and within the gate slots were especially erratic.

It was also observed that when the head at some locations on the bottom beam increased, the head at other locations decreased. There was no periodicity to the fluctuations, however. The supposition of an unstable eddy formation beneath the gate and within the gate slots provides a possible explanation for the observed behavior.

For the most part the fluctuations were reasonable, amounting to only a few hundredths of a foot, model. Frequently, however, the heads on the bottom of the roller extensions and within the gate slots fluctuated by several 10ths of a foot, and on rare occasions they fluctuated as much as 2 feet, model.

The severest fluctuations were encountered when operating at the cavitation threshold, especially when the flow was on the verge of becoming ventilated from the end of the tunnel, for then both the downstream pressure and the tank pressure fluctuated badly. For free discharge at the gate, large fluctuations were observed in the 70- to 90-percent range of gate openings. For free discharge downstream from the transition section and with the smallest of the lip extensions, there were large fluctuations at the 90-percent gate opening.

In view of the nature of the fluctuations, particularly their compensating characteristics, the manometer board was photographed in a more or less random manner. Care was taken, however, not to photograph an extreme condition. The results obtained by the procedure were satisfactory and plotted as reasonably smooth and reproducible curves.

Computation of Results

The piezometers on the bellmouth were observed during the first series of tests ($e/d=0.8$); but since nothing of a disturbing nature was detected (except as noted below), their observation was discontinued. The exception was the erratic fluctuation of piezometer 61 (and occasionally piezometer 62) when the flow rate was high. These piezometers are identified in figure 8. The fluctuations can be attributed to the re-entrant-type flow that occurs around the baseplate of the model. The trashrack foundation will prevent this type of flow from occurring in the prototype.

To compute the downpull all manometer read-

ings were converted to piezometric heads relative to the tunnel invert at the gate. To each external surface area of the gate having a horizontal projection, a mean piezometric head was assigned based on the measured values. Products of these heads and areas were summed algebraically with top areas being taken as positive and bottom areas as negative. Their total was multiplied by the specific weight of water to obtain the model downpull. Details of these calculations are given in the appendix.

In associating piezometric heads and areas certain arbitrary assumptions had to be made. Only three piezometers were located on top of the gate (fig. 7): No. 27 on the top beam near, but not in a gate slot, No. 26 on the skinplate on the gate centerline, and No. 25 on the skinplate at the same lateral location as No. 27. With no flow passing over the top of the gate all three piezometers indicated essentially the same head as was measured by the piezometers in the gate well (bonnet head). When flow over the top of the gate occurred, the three piezometers indicated different heads, all of which were slightly less than the bonnet head (fig. 10).

One might expect the piezometer on the top beam to always indicate a higher head than the two at the top of the skinplate. The expectation, however, was seldom borne out by observation due, no doubt, to the three-dimensional character of the flow. The head indicated by piezometer 27 was generally between the heads for 25 and 26. In view of these observations, the arithmetic mean of the three piezometric heads was used with the entire top area of the gate including the projections of the side seals and roller trains.

There were no piezometers under the top seal. It was assumed that with flow over the top of the gate the heads above and below the top seal would be equal and there would be no contribution to downpull. With no flow over the top of the gate it was assumed that the head beneath the top seal was equal to the head downstream from the gate when the gate was submerged. For free and air-vented discharges the pressure head beneath the top seal was the same as the pressure head downstream from the gate. The head downstream from the gate was measured by piezometer 28. The head on top of the top seal was taken to be the same as on top of the gate. Head differentials across the seal contributed to downpull on the gate and were taken into account in the downpull computations.

Pressures on top of the bottom seal were not measured on the model. Although the area involved is small compared with the total gate area, the associated force component can be significant under some operating conditions. For free and air-vented discharges and with gate openings greater than 10 percent (and less than 90 percent after revision of the recess) a high-velocity jet from the gate well flowed down the downstream face of the gate leaf and impinged on the top of the bottom seal. Under these conditions the head on top of the seal was assumed to be equal to the average head on top of the gate. Use of this head, which was somewhat less than the bonnet head, tended to compensate for unknown losses in the jet.

With free discharge downstream from the transition section, the gate was submerged for gate openings greater than 60 percent. Nevertheless, it was assumed that the bottom seal was close enough to the slot from which the gate well jet issued for the head on top of the seal to be significantly influenced by the jet. The head on top of the seal was computed in the same way as for free and air-vented discharges.

In spite of low downstream pressures when the cavitation threshold was simulated, the pressures under the gate lip remained above the model vapor pressure. This indicated that the gate lip was effectively screened from the region of prototype cavitation by the jet flowing down the gate leaf. The measured values of head beneath the lip were therefore used in computing the downpull.

For gate openings less than 20 percent (and greater than 80 percent with the revised recess) the top seal prohibited flow down the face of the gate leaf, and the pressure on top of the bottom seal was considered equal to the pressure indicated by piezometer 28.

When the model was operated with a back pressure to simulate the flow for maximum power generation, the bottom seal was generally submerged. For gate openings of 70 percent and greater the flow from the bonnet was negligible, and for smaller gate openings it was assumed that the jet was sufficiently dissipated for its effect on the bottom seal to be negligible. Under these conditions the heads above and below the bottom seal were assumed to be equal.

For controlled discharge flow and for a gate opening of 3.6 percent the pressure downstream from the gate was negative. On some tests the air vents were then opened and a hydraulic jump that submerged the gate lip was formed in the transition section (fig. 11A). The downpull on the bottom seal

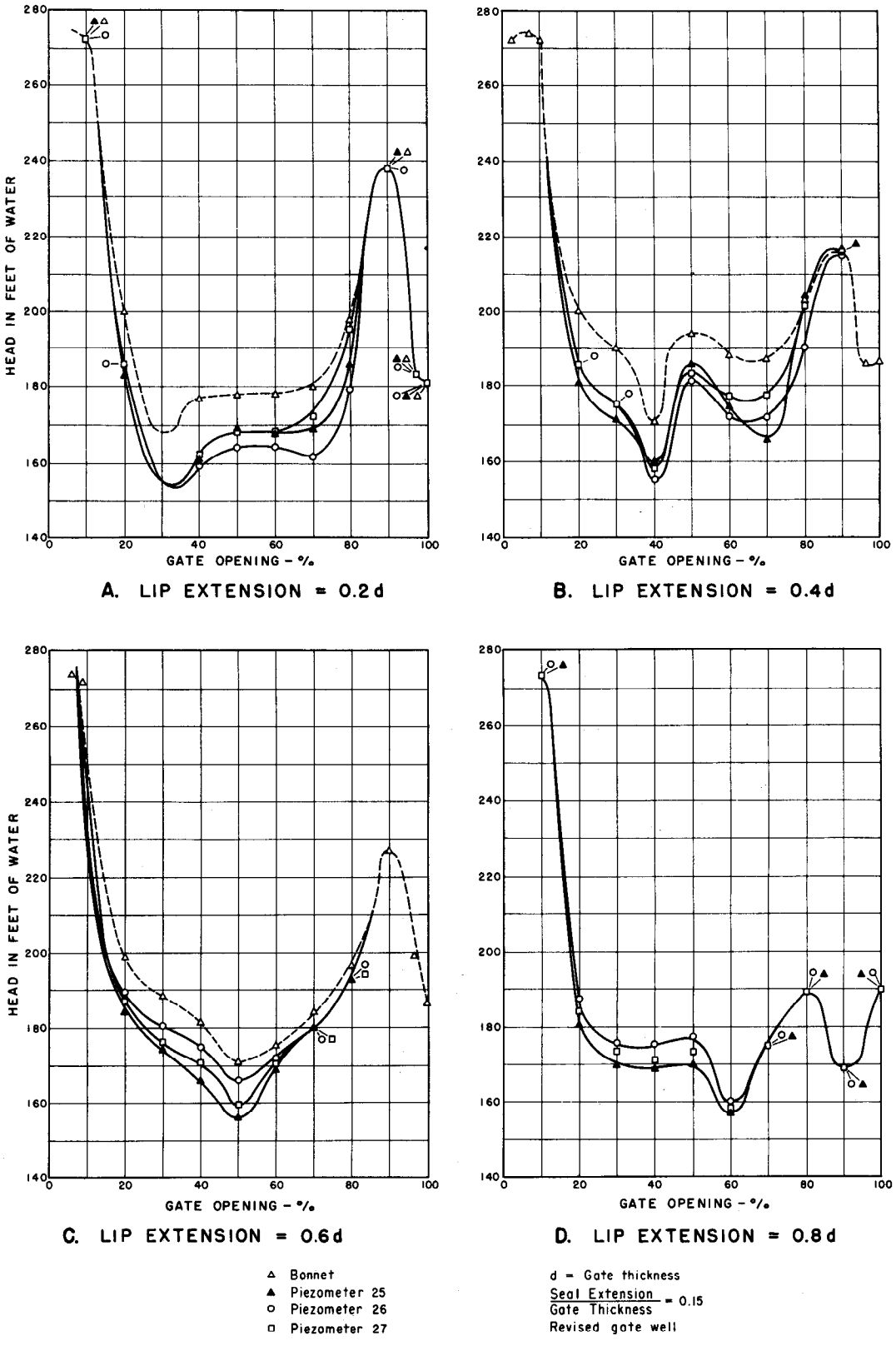

FIGURE 10.—Bonnet head and pressure distribution on top of gate leaf.

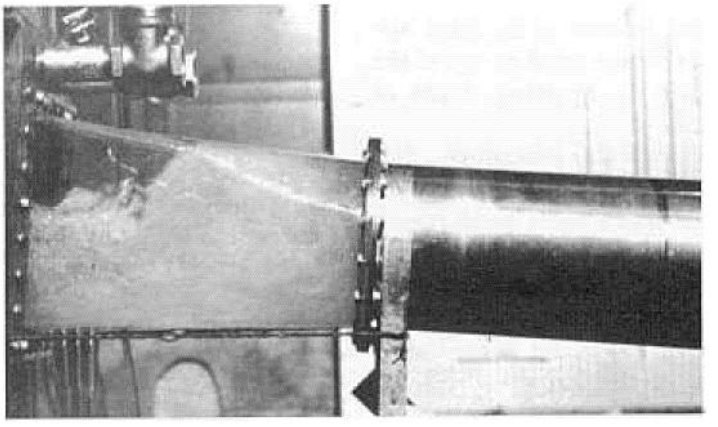

A. In certain tests with controlled discharge conditions with the air vents open, a jump that submerged the gate lip was formed in the transition section.

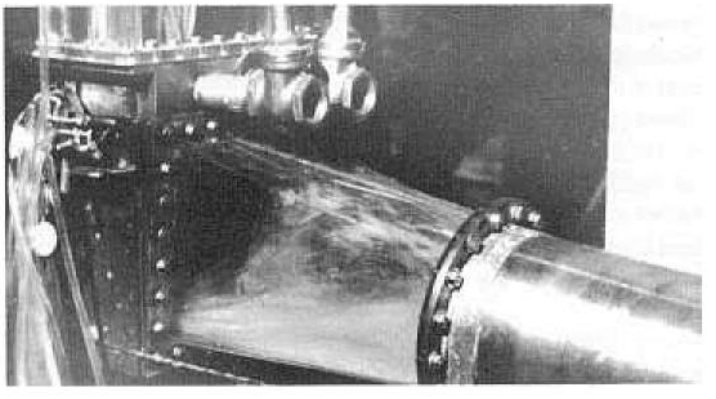

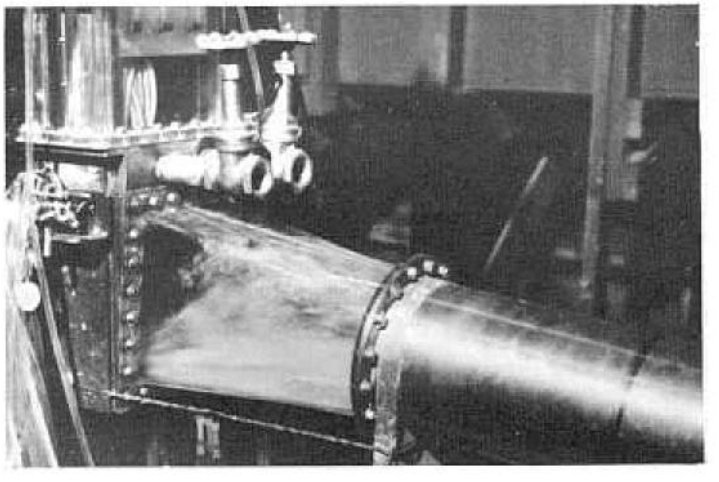

B. At smaller gate openings ventilation occurred from downstream, as well as through the vents, and a fluctuating, continuously free discharge condition prevailed. Opening = 7%, $e/d = 0.4$.

FIGURE 11.—Open-channel flow conditions downstream from gate at small openings.

was computed in the same manner as for other air-vented discharges except that the head on top of the seal was computed taking the apparent depth of submergence into account.

There was one exception to this procedure. For $e/d=0.8$ the hydraulic jump had not been observed because at the time of the tests a sheet metal transition section was being used. As a result, no correction was made for the depth of submergence. The effect of submergence was considered to be so small that the computations were not revised after discovering the presence of the jump.

The head on the bottom of the side seals and on the portion of the gate lip and bottom seal that was within the gate slot was assumed to be the arithmetic mean of the heads on the gate lip and on the bottom of the roller extension.

The pressure distributions under the bottom beam of the gate leaf for emergency closures with 0.6 and 0.4d lip extensions are shown in figure 12. The effect of three-dimensional flow is clearly evident. In regions of maximum downpull the pressures near the sides of the gate are much higher than on the centerline. In regions of uplift the reverse is true. Assuming that the pressures on the centerline are characteristic of two-dimensional flow, it can be concluded that both downpull and uplift are reduced with three-dimensional flow.

The head in the reservoir (pressure tank) was measured directly. For submerged discharge at the gate the piezometric head of the contracted jet was assumed to be the same as the head indicated by piezometer 28. For free and vented discharge it was taken as the depth of water at the contracted section plus the pressure head indicated by piezometer 28. The depth of the jet for vented discharges was assumed to be the same as for free discharge at the same gate opening. Free discharge depths were measured with a point gage except for $e/d=0.8$. For this lip extension a coefficient of contraction curve was assumed.

With the net head across the gate denoted by HN, the downpull coefficient can be expressed as

$$K=\frac{P}{A\alpha HN}, \tag{6}$$

α being the specific weight of water and A being the product of gate width and thickness. According to equation 5, the downpull coefficient has the same value for model and prototype when y/y_o and e/d have the same values for model and prototype.

Using subscripts m and p to denote model and prototype respectively,

$$P_p=P_m\left(\frac{A_b\,(HN)_p}{A_m(HN)_m}\right). \tag{7}$$

With H as the reservoir head and h as the head in the contracted jet, $HN=H-h$, equation 7 can now be expressed as

$$P_p=P_m\left(\frac{(A_p)}{(A_m)}\,\frac{(H_p)}{(H_m)}\,\frac{1-(h/H)_p}{1-(h/H)_m}\right).$$

If the relationship between H and h is governed by potential flow,

$$(h/H)_p=(h/H)_m$$

and

$$P_p=P_m\left(\frac{A_p}{A_m}\,\frac{H_p}{H_m}\right). \tag{8}$$

As closely as possible the reservoir head in the model was set at 7.80 feet, which is the model scale equivalent of a 273-foot prototype head. To compensate for small differences the following substitution was made:

$$H_m\times\frac{7.80}{7.80}\times\frac{H_p}{273}$$

$$\frac{H_p}{H_m}=\frac{35(7.80)}{H_m}.$$

Equation 8 now becomes

$$P_p=(35)^3P_m\,\frac{(7.80)}{H_m}$$

$$=42{,}875P_m\,\frac{(7.80)}{H_m}. \tag{9}$$

In the first series of tests, $e/d=0.8$, the head downstream from the gate fell below the cavitation threshold. To compute the prototype downpull for this condition it was assumed that the downpull would be proportional to the net head. The correction factor of $7.80/H_m$ in equation 9 was therefore replaced by (HNP/HN) in which HN is the measured net head for the model and HNP is the net head that would have been held at the cavitation threshold.

To carry out all of the computations described above, a computer program was written in the FORTRAN language for a 7090 computer. This program is included in the appendix.

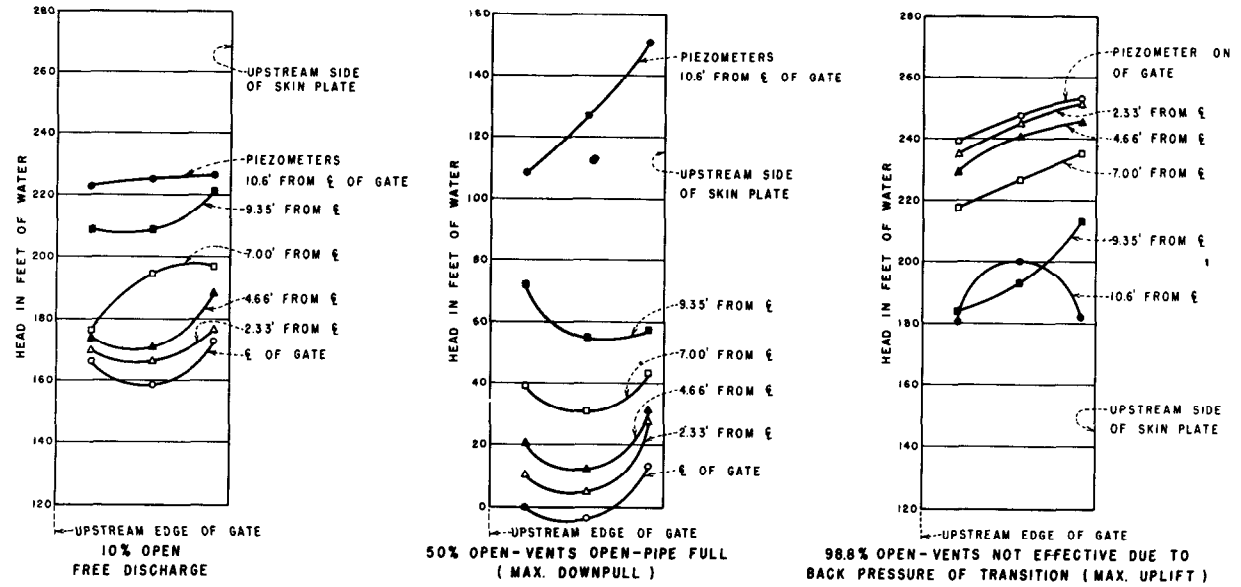

A. LIP EXTENSION = 0.4 d

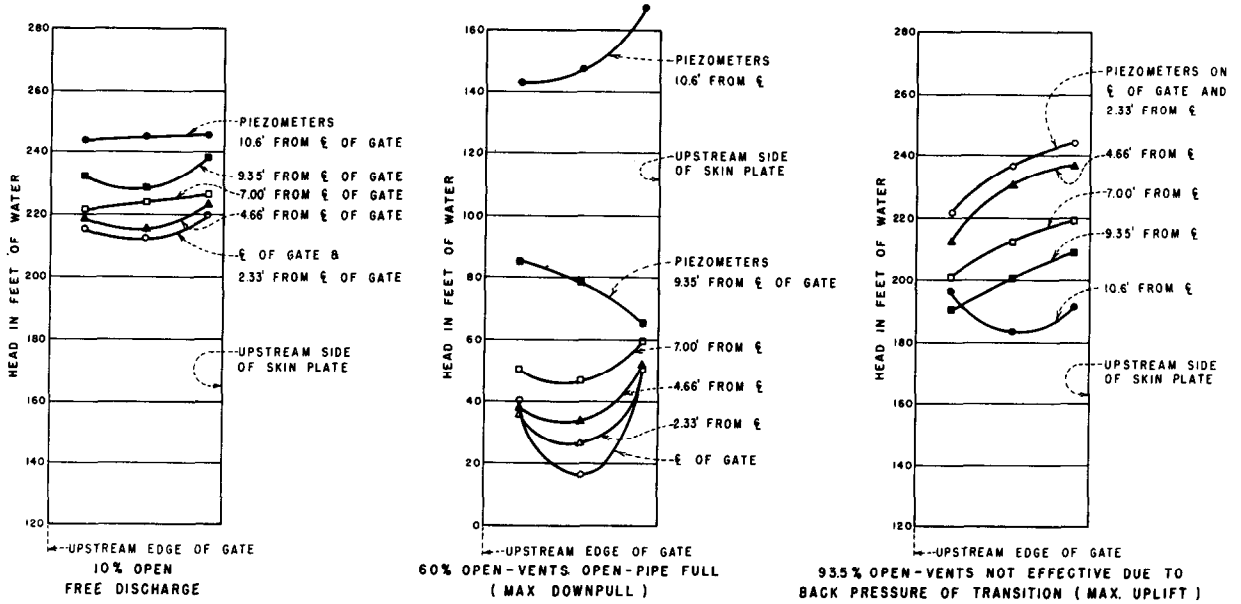

B. LIP EXTENSION = 0.6 d

d = GATE THICKNESS

FIGURE 12.—Pressure distribution on bottom of gate leaf.

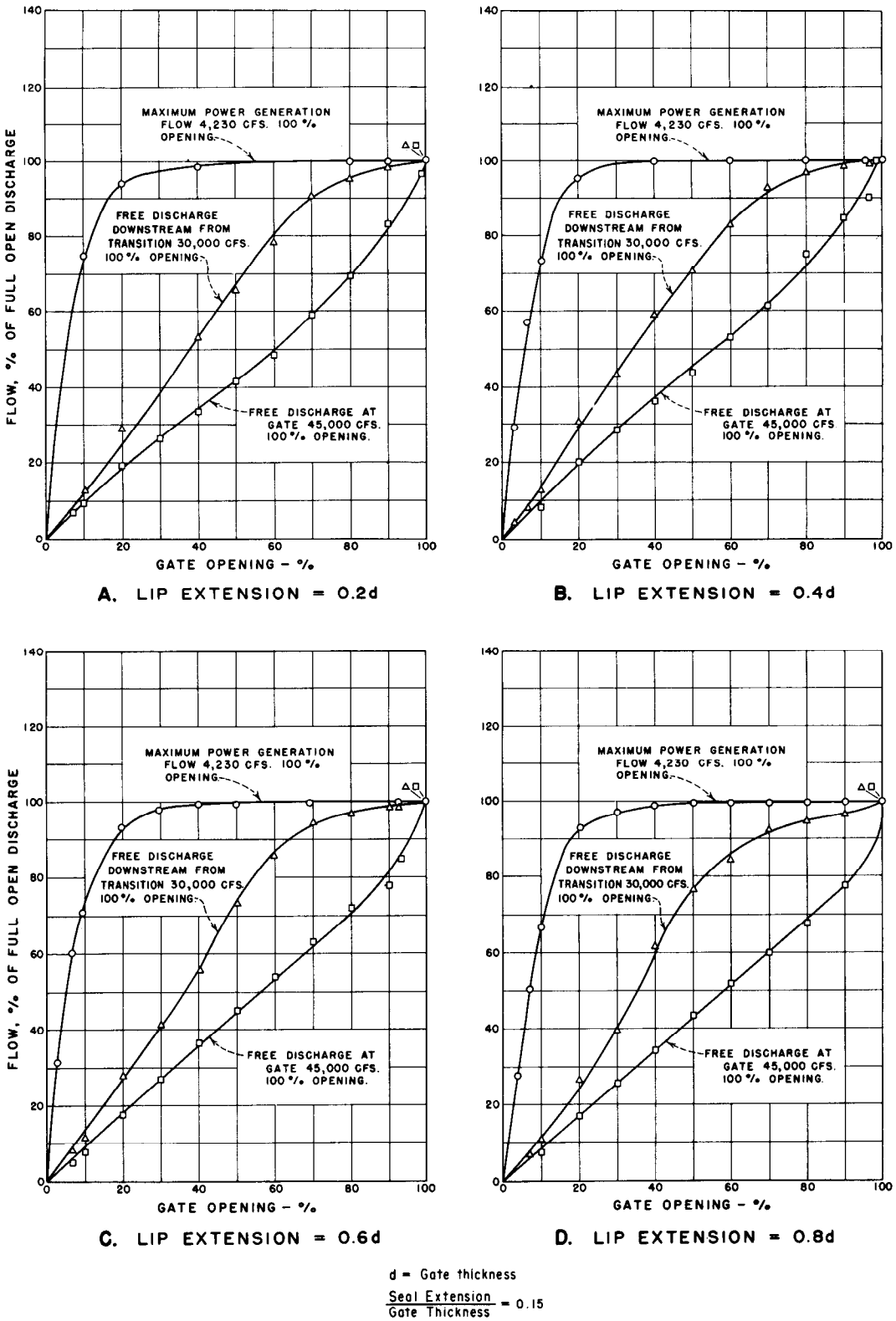

FIGURE 13.—Flow rates versus gate opening and operating conditions.

The flow rate information obtained from the model study is presented in figure 13 as a percent of the flow for a wide open gate. In computing points for these curves the measured flow rates were adjusted to what they would have been if the reservoir head had been the model scale equivalent of 273 feet. To do this it was assumed that for the small corrections involved

$$Q^1=Q\sqrt{\frac{7.80}{H}}. \tag{10}$$

Here Q^1 is the adjusted flow rate, Q is the measured flow rate, and H is the measured reservoir head.

The prototype flow rates corresponding to 100 percent gate openings were computed in the following manner. In the equation

$$Q=CA\sqrt{2gH},$$

C was assumed to have the same value for model and prototype under corresponding operating conditions. It follows immediately that

$$Q_p=Q_m\left(\frac{A_p}{A_m}\left(\frac{H_p}{H_m}\right)^{1/2}\right).$$

With the head ratio equal to the model scale ratio,

$$Q_p=(35)^{2.5}Q_m=7250Q_m. \tag{11}$$

RESULTS

Flow Rates

Curves giving the flow rate as a function of gate opening for each flow condition and lip extension are presented in figure 13. The curves for each flow condition are radically different, but the effect of lip extension is almost negligible.

For flows simulating maximum power generation the flow rate was nearly constant for the first 50 percent of gate closure. Control then gradually shifted to the gate, and for the last 20 percent of closure, control was exercised almost entirely by the gate.

With free discharge downstream from the transition section, control gradually shifted from the transition section to the gate as the gate was closed. From the 60-percent open position to complete closure, the gate had full control except for the effect of air supply.

For completely free discharge the gate was the only control, and the flow rate was very nearly a linear function of gate opening. The increased slope for gate openings between 90 and 100 percent is probably due to a reduction in the jet contraction.

General Downpull Characteristics

The curves in figure 2 give the computed prototype downpull as a function of gate opening for each flow condition and lip extension. In figure 2A, curves for each flow condition with the single lip extension of $e/d=0.8$ are presented. In figures 2B, C, and D, families of curves for different flow conditions with e/d as the parameter are presented.

All of the curves clearly show the effect of the offsets and recess in the downstream wall of the gate well (fig. 3). With the gate fully closed the downpull was entirely due to the difference in head across the top seal. As the gate was started upward from the closed position, the head on the bottom of the gate decreased while the head on top remained high. The downpull increased. But at gate openings of about 10 percent the top seal reached the top of the lower offset and seal seat and began moving into the region of the recess. This allowed flow to pass out of the gate well, downward behind the gate and into the downstream conduit. As a result, the head on top of the gate decreased and downpull diminished. At a 20-percent opening the seal was well within the recessed area and enough flow occurred over the top of the gate to significantly reduce the head in the gate well and on top of the gate (fig. 10). The net effect was a large reduction of downpull. In fact, for $e/d=0.8$, an uplift was encountered at a 20-percent gate opening (figs. 2B and C).

As the gate was opened more, the downpull again increased due to a further reduction of head beneath the gate. There were two exceptions. For flows representing maximum power generation the downpull did not increase, but decreased for $e/d=0.2$ and 0.4, and increased only slightly for $e/d=0.8$ (fig. 2B). These actions, at maximum power generation flows, were due to the shift of control from the gate to the hollow-jet valve (representing the penstock and turbine back pressure) and to the reduction in net head across the gate.

For both types of free discharge, maximum values of downpull occurred in the 10- and 90-percent range of gate openings for $e/d=0.2$, and in the 50- to 80-percent range for the other e/d ratios. For $e/d=0.4$ and 0.6, these maximums were greater than the maximums encountered at 10 percent gate openings.

The rapid reduction of downpull at gate openings greater than those at which maximum downpulls were observed is due primarily to the increase in head beneath the gate. This increase in head is probably due to a reduction of flow curvature at the upstream edge of the gate bottom as the bottom of the gate moves closer to the crown of the tunnel.

For all flow conditions and lip extensions an uplift was observed in the 90- to 100-percent range of gate openings. For both types of free discharge the uplift was severe. The uplift was caused by the simultaneous reduction of head in the gate well and increase of head beneath the gate as the bottom

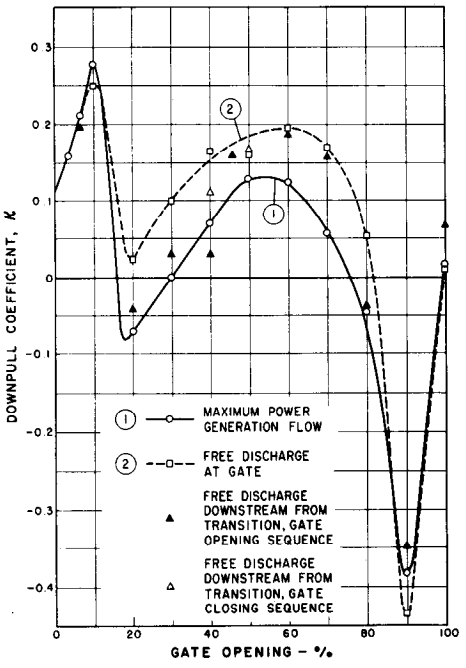

A. EFFECT OF VARIOUS OPERATING CONDITIONS - $\%_d = 0.8$

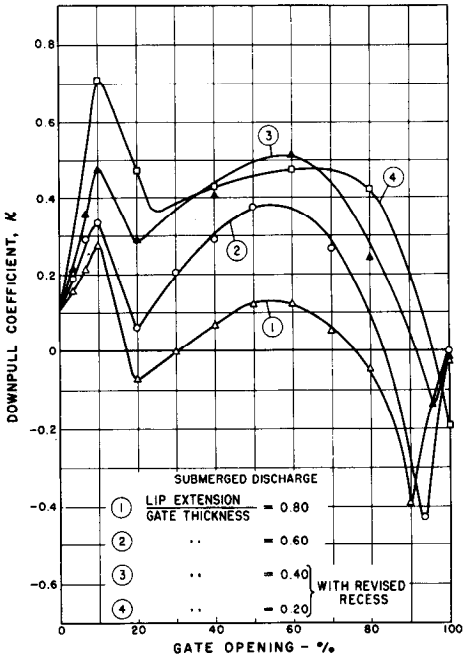

B. EFFECT OF LIP EXTENSIONS- MAXIMUM POWER GENERATION FLOW
Q = 4230 C.F.S.

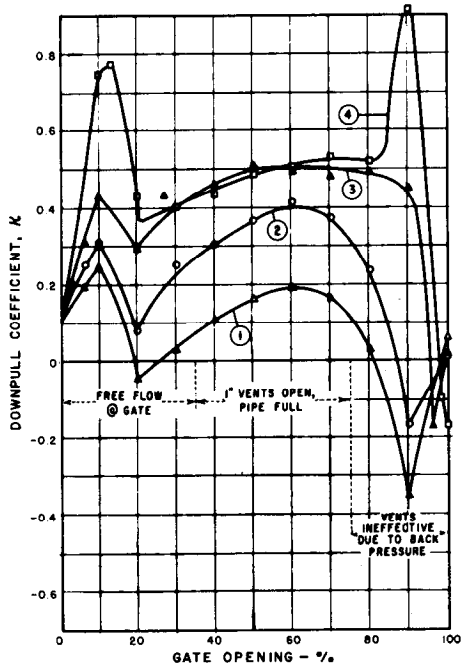

C. EFFECT OF LIP EXTENSIONS- FREE DISCHARGE DOWNSTREAM FROM TRANSITION
Q = 30 000 C.F.S.

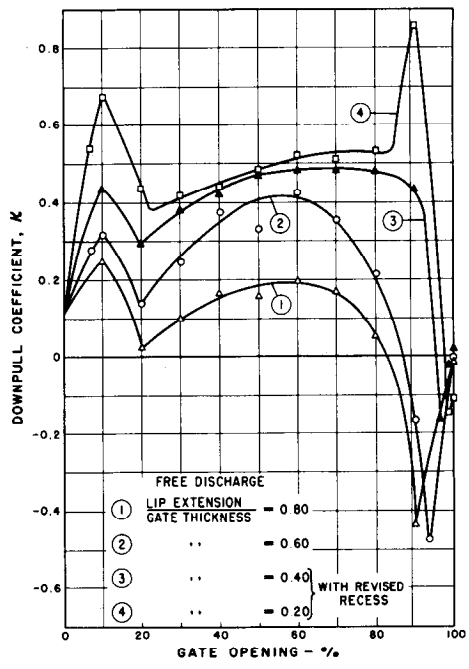

D. EFFECT OF LIP EXTENSIONS- FREE DISCHARGE AT GATE
Q = 45 000 C.F.S.

$K = \frac{\text{Downpull}}{A\ \gamma\ HN}$ where: A = Cross-sectional area of leaf.
γ = Sp. wgt. of water, 62.4 #/ft.^{3}
HN = Net Head across gate - feet of water.

$\frac{\text{Seal Extension}}{\text{Gate Thickness}} = 0.15$

FIGURE 14.—Downpull coefficients.

beam of the gate moved into the gate well. When the body of the gate extends sufficiently into the tunnel, for instance at a 75-percent opening, the flow approaching the gate is divided by the obstruction of the leaf, and part passes upward in front of the leaf to enter the bonnet while the rest turns downward to pass under the leaf. Thus, there is a stagnation point on the upstream side of the gate. As the gate approaches the full open position, the stagnation point shifts from the front of the gate to the lip extension or to some region along the bottom beam. The result is a reduced tendency for water to enter the bonnet, and an increased tendency for higher pressures to occur on the bottom beam of the gate leaf.

After evaluating the first two series of tests ($e/d=0.8$ and 0.6) where uplift was found to be a problem, the recess in the gate well was revised. A second offset was placed on the downstream wall at a point where the top seal of the gate reached it at an 88 percent gate opening (fig. 3). A clearance equivalent to 1 inch prototype was maintained between the seal and the face of this second offset. This design effectively blocked most of the flow from passing over the top of the gate for gate openings larger than 88 percent and produced a significant increase in the bonnet head to counteract the fairly high leaf bottom pressures. The uplift was greatly reduced, as can be seen from a comparison of curves 2 and 2′ in figures 2 and 4. The revised recess was used in all subsequent tests.

San Luis Prototype Gate Downpull

A lip extension of 27 inches, or an e/d ratio of 0.55 was selected as the best for the San Luis gates after taking into consideration allowable downpull and uplift forces and the formidable structural problems involved in supporting large extensions. By interpolation between the downpull curves obtained for e/d ratios of 0.4 and 0.6, the maximum prototype gate downpull forces for the San Luis gates were computed to be 405 kips for maximum power generation flow, 800 kips for a severe break in the penstock, and 710 kips for free discharge conditions at the downstream gate frame (fig. 2).

Downpull Coefficients

The dimensionless downpull coefficients for $e/d=0.8$ were determined for submerged and free discharge conditions, and for free discharge downstream from the transition section (fig. 14A). Curves of the downpull coefficients for the various discharge conditions are also presented with e/d as a parameter (fig. 14B, C, and D). By using these dimensionless coefficients, K, in the equation, Downpull$=KA\alpha\ (HN)$, the downpull for any geometrically similar gate can be computed. In this equation A is the cross-sectional area of the gate, α is specific weight of water, and HN is the net head across the gate.

All the curves have the same general shape except at the large gate openings. The difference between the downpull coefficient curves for controlled discharge and the prototype downpull curves for the same condition is due to the influence of the net head across the gate that appears in the denominator of the downpull coefficient. For controlled discharge the variation of net head with gate opening was very large, whereas for free discharge it was relatively small.

The downpull coefficients for free discharge downstream from the transition section agree remarkably well with the coefficients for free discharge at the gate (fig. 14C and D). The greatest deviation is in the 20- to 60-percent range of gate openings for which the pressure downstream from the gate was subatmospheric. The agreement at large gate openings is noteworthy, for here the discharge was submerged rather than free.

There is also fair agreement between the downpull coefficients for free discharge downstream from the transition section and the downpull coefficients for submerged discharge (fig. 14B and C). The greatest discrepancy here is in the range of gate openings from 60 to 90 percent. In this range the net head across the gate for controlled discharge was very small and was determined by taking the difference of two relatively large values. The surprising features are that the agreement is as good as it is and that the points for the submerged discharge downpull coefficients plot as smoothly as they do.

Air Requirements

Measurement of the quantity of air that must be admitted downstream from each San Luis outlet works gate to maintain ambient pressures above the cavitation range during emergency closures were required so that properly sized air vents could be provided in the structures. Information was obtained from the model for one, three-fourths, and one-half atmospheres of negative (or subatmos-

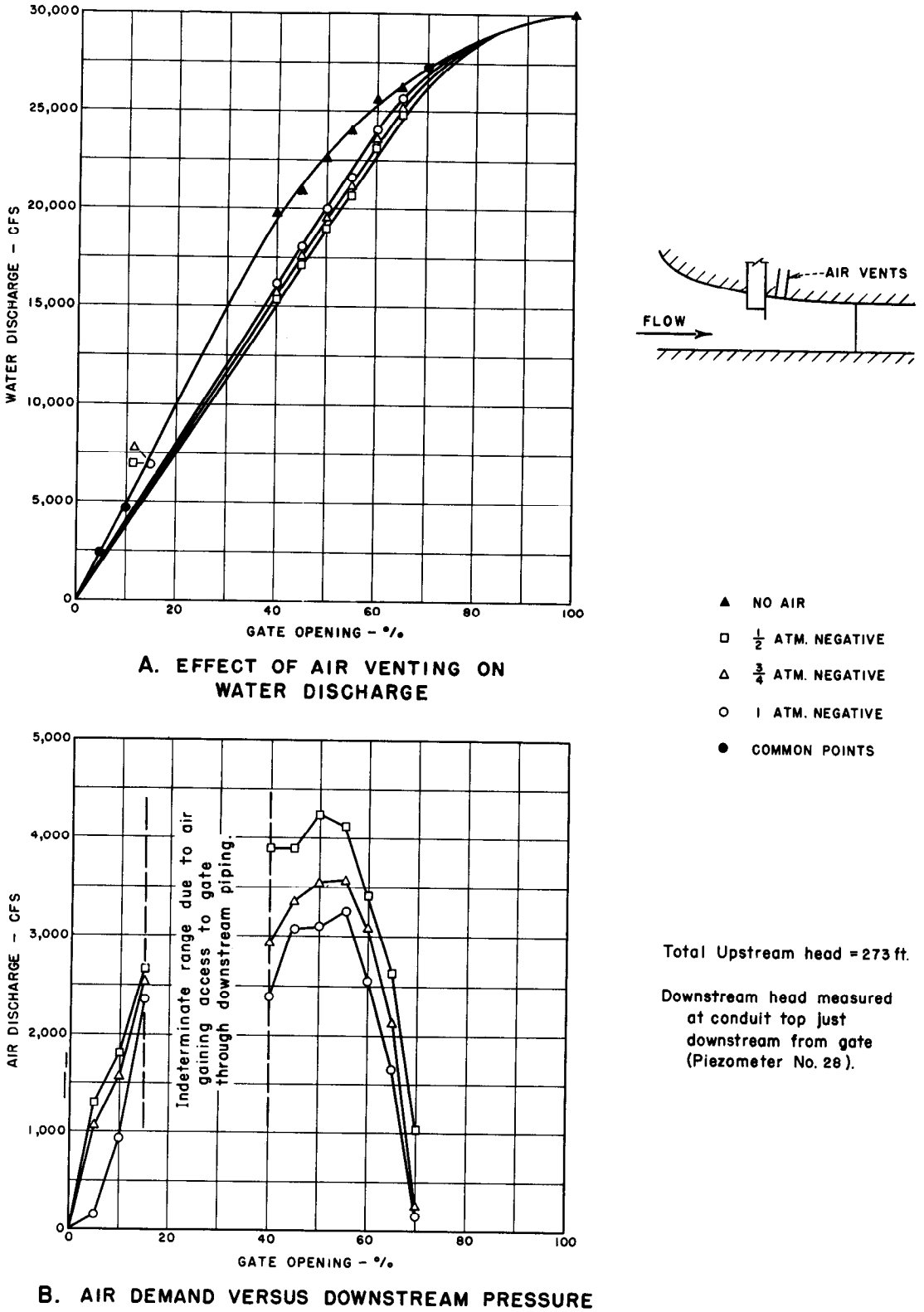

A. EFFECT OF AIR VENTING ON WATER DISCHARGE

B. AIR DEMAND VERSUS DOWNSTREAM PRESSURE

FIGURE 15.—Air demand and effect of downstream pressure on discharge.

pheric) pressure measured at the top of the conduit just downstream from the gate (piezometer 28). Sharp edged orifice plates ranging in size from ½ to 1½ inches in diameter were used in conjunction with a U-tube water manometer to measure the airflow into the model. A tank head representing 273 feet prototype was maintained for all tests. The negative head for no air supplied was recorded for each gate position. Air vents were then opened until negative pressures equal to one, three-fourths, and one-half atmosphere (prototype) were recorded downstream from the gate. Adjustments in the discharge were necessary to maintain the appropriate model tank head for each downstream negative pressure (fig. 15A). The downstream conduit was equipped with the hollow-jet valve in an attempt to prevent venting from the downstream conduit when operating the outlet works gate at openings below 40 percent. The pressure head in the downstream conduit for gate openings below 40 percent also was recorded.

The prototype air demand was obtained by multiplying the model air demand by the model-to-prototype length ratio raised to the 5/2 power. This relationship as a criteria for air demand is not yet supported by accurate field data, but must be assumed to provide a satisfactory approach to the problem pending further field tests and model-prototype correlations. Refinements, such as the effects of compressibility, were not considered.

The data showed that the maximum air requirements occurred with a subatmospheric pressure of one-half atmosphere (fig. 15B). The peak demand occurred between the 50 and 55 percent gate openings and was 4,250 c.f.s. This value should be used for design purposes. Higher air discharges would, of course, be required if pressures nearer atmospheric were required downstream from the gate. A value of one-half atmosphere subatmospheric was considered acceptable for this installation because emergency operations which require air will be infrequent and of short duration.

Data on air demand were unobtainable between gate openings of 15 and 40 percent (fig. 15B) with the model arrangement using the hollow-jet valve for back pressure control. When settings were attempted at these gate openings, air would intermittently be drawn upstream through the top portions of the hollow-jet valve to upset the flow conditions and change the readings. Readings were difficult but possible at 15 percent and smaller openings. However, the degree of reliability of these data is less than for data obtained at openings greater than 40 percent.

Tests by the Corps of Engineers at Pine Flat Dam indicated a secondary air demand peak at about a 5-percent gate opening.[1] A similar peak was sought in the San Luis model gate, but could not be determined because of the operational difficulties at small openings.

Major modifications to the model would have been required to obtain more accurate air demand data for small gate openings, and it was felt that a secondary peak, should one occur, would not appreciably exceed the primary peak. The time-consuming modifications and additional testing were considered unjustified and were not undertaken.

[1] "Hydraulic Design Criteria," Corps of Engineers, Chart 050–1/1.

DISCUSSION

Effect of Flow Conditions

The downpull for controlled (submerged) discharge is much less than for free discharge, and its variation with gate opening is quite different. Nevertheless, the downpull coefficient curves for controlled discharge and for free discharge are very similar. In view of the uncertainty in the downpull coefficients for controlled discharge, and in view of the good agreement between the coefficients for free discharge at the gate, and for free discharge downstream from the transition when the latter produced submerged discharges at the gate, it can be speculated that a single family of curves valid for both free and submerged discharges can be developed. Additional tests of submerged discharges with larger net heads across the gate are required to substantiate the speculation.

Effect of Lip Extension

The maximum downpull increased with every reduction of lip extension (fig. 4A). The maximum uplift increased with decreasing lip extensions until the e/d ratio reached a value of 0.4. For $e/d=0.2$ the maximum uplift was somewhat less than for $e/d=0.4$.

Effect of Shaft Wall Recess

The recess in the downstream wall of the gate well was extremely effective in reducing downpull. The revision of the recess to prevent flow over the top of the gate in the 90- to 100-percent range of gate openings was also effective in reducing uplift. The recess is expected to be somewhat less effective in both respects if the extension of the seals is decreased.

Three-Dimensional Effects

The presence of sidewalls and flows in the gate slots definitely affected the pressures on the bottom beam of the gate (fig. 12). These effects are sufficiently large to be a significant factor in computing downpull forces.

Experimental Accuracy

Because of the many assumptions that were made in computing the model downpull and because detailed information on the random fluctuations of piezometric heads is lacking, no reliable estimate of experimental accuracy can be made. Probably the greatest source of uncertainty is in the use of the arithmetic mean of only three piezometer readings to determine the effective head on top of the gate. Undoubtedly the effective head is less than the bonnet head, but it may be more than the mean value that was used. For gate openings less than 20 percent and greater than 80 percent, the difference between the bonnet head and the head on top of the gate was negligible; in the middle range of gate openings the difference was approximately constant. Using half of the maximum difference in heads to compute a possible increase in downpull, an increase of approximately 50 kips is obtained for the middle range of gate openings. This is probably a conservative estimate and a more reasonable correction is something less than 50 kips.

Fortunately the piezometric heads exhibiting the greatest fluctuations were associated with relatively small areas of the gate. It is estimated that the uncertainty in downpull due to fluctuations in piezometer readings is much less than 50 kips. In view of the conservative estimate of the uncertainty in head at the top of the gate, an estimate of 50 kips for the overall probable error in downpull seems reasonable.

Using the above estimate of probable error in downpull and assuming a 1-percent uncertainty in the net head across the gate for free discharge, a probable error of plus or minus 3 percent in the free-discharge downpull coefficients is obtained.

Because of the very large uncertainty in the net head across the gate for controlled discharge (in some cases the uncertainty is as much as 50 percent), no significant estimate of probable error for the submerged-discharge downpull coefficient can be made.

The peak in downpull at 90 percent gate opening for $e/d=0.2$ might appear to be attributed to a gross

experimental error. However, since the peak occurs in two independent tests (free discharge and free discharge downstream from the transition section), its existence is undoubtedly real. It can be traced to a sudden increase in bonnet head which was probably caused by the body of the gate extending farther into the flow for this lip extension than any of the others at the same gate opening.

Comparison With Other Investigations

The work of two other investigators has been presented in a nondimensional form that makes direct comparison with the results of this investigation feasible. It must be pointed out, however, that in neither case is there complete geometric similarity with the installation reported on here.

H. E. Kobus, under the direction of Professor Naudascher at the State University of Iowa, studied the downpull on high headgates for the special case of a two-dimensional submerged discharge flow without a recess in the downstream wall of the gate well.[2] The upstream edges of these gate leaves were well rounded ($r/d=0.4$).

For $e/d=0.6$, Kobus found a maximum downpull coefficient of 0.46 at a 40-percent gate opening. This can be compared with a maximum value of 0.42 for free discharge at a 57-percent gate opening of the San Luis gate and with a value of 0.38 for submerged discharge. However, it can be estimated that values as high as 0.68 and 0.82 for free and submerged discharge, respectively, might have been obtained if there had been no recess in the gate well.

By interpolation, values for other lip extensions can be determined from Kobus' work. For $e/d=0.4$, $K=0.72$. Comparable values for the San Luis gate are 0.49 and 0.51 for free and submerged discharge, respectively. With an estimated correction for the effect of the recess, these values go up to 0.78 and 0.88.

For $e/d=0.2$ on the San Luis gate, the maximum values of the downpull coefficients are 0.85 and 0.71 for free and submerged discharge, respectively. With an estimated correction for the effect of the recess, the values change to 1.01 and 1.10 at 75 and 65 percent gate openings, respectively. The corresponding value from the work of Kobus is 0.94 at a 30-percent gate opening.

P. M. Smith, working for the U.S. Army Corps of Engineers, studied the downpull on the Ice Harbor powerhouse gate.[3] His study was three dimensional and included a recess in the downstream wall of the gate well, but his gate featured a combination of sloping bottom and extended lip designs. For this reason, a direct comparison with e/d values for the San Luis gate is not possible. Maximum values of the downpull coefficient ranged from 0.92 to 1.16, the downpull increasing with decreasing lip extensions.

The downpull coefficients reported by both Kobus and Smith are based only on the top and bottom beams of the gates. They do not include the effects on downpull of the seals, rollers, or the gate lip.

Use of Downpull Coefficients In Design

The downpull coefficients presented in this report, particularly the ones for free discharge, can be used for high-head installations that are geometrically similar to the San Luis installation. In using the coefficients a reasonable estimate of the velocity head in the contracted jet issuing from beneath the gate must be made. This estimate can be based on flow rate information if contraction coefficients for the gate are known. Curves of contraction coefficient vs. gate opening with e/d as a parameter are given in figure 4B. Flow rate information will, of course, depend on the particular installation.

[2] "Effect of Lip Shape Upon Hydraulic Forces on High Head Gates," a thesis by H. E. Kobus, State University of Iowa, February 1963.

[3] "Hydraulic Downpull on Ice Harbor Powerhouse Gate," by Peter M. Smith; a paper presented at the May 1963 ASCE Water Resources Engineering Conference in Milwaukee, Wis.

APPLICATION OF RESULTS

Problem.—Find the maximum downpull during closure of a 10.0- by 18.0-foot gate with a 200-foot operating head and a severe conduit rupture immediately downstream from the transition. The gate installation is similar to the San Luis installation; the thickness, d, is 2.5 feet; and the lip extension ratio, e/d, is 0.5.

Solution.—Using figure 14C and interpolating between the curves for $e/d=0.4$ and 0.6, the maximum downpull coefficient, K, is 0.45 at a 61-percent opening.

The gate, which closes an opening 10.0 feet wide, extends into the slots 1.5 feet on each side to produce a total length of 13.0 feet. The cross-sectional area is 2.5 by 13.0, or 32.5 feet^2.

The net head, HN, across the gate at this discharge condition is 200 plus 15=215 feet, assuming a subatmospheric pressure of about one-half atmosphere downstream from the gate.

Using the equation from figure 14,

$$\begin{aligned} \textit{Maximum downpull} &= KA_{\alpha}HN \\ &= 0.45\ (32.5)\ (62.4\ (215) \\ &= 196{,}000 \text{ pounds} \\ &= 196 \text{ kips.} \end{aligned}$$

APPENDIX

A digital computer performed most of the computations involved in transforming raw data into the equivalent downpull forces on the gate leaf. The manometer readings were first converted to net piezometer heads referred to the gate invert. Specific net heads were then multiplied by the appropriate external surface areas of the gate having a horizontal projection. These products were summed algebraically with top areas being taken as positive and bottom areas as negative. Their total was multiplied by the specific weight of water to obtain the downpull force in pounds.

A flow diagram of the computer program, definitions of the symbols used, the program itself, and a sample of computer printout follow.

Symbols Used in Computer Program:

$A(i)$	i=1–8 Areas
$HR(i)$	i=1–28 Piezometer readings, from photographs
$H(i)$	i=1–28 Head relative to invert (computed by computer)
NEX	number of lip extension 1 is e/d=0.8 2 is e/d=0.6 3 is e/d=0.4 4 is e/d=0.2
NGO	number of gate opening (1 is wide open)
NFC	number of flow condition (see below)
$HEAD$	tank head, from data sheet
J	an index to make printout go to top of next page
B, C, D	mercury readings for sections of piezometer board (see below)
E, F, G	elevation differences used in computations (see below)
K	index to adjust for location of Piezometers 16 and 17
AV1, 2, etc.	averages computed by computer (see computer program)
DPM	model downpull
HN	net head
CF	downpull coefficient
HNP	adjusted net head
DPP	prototype downpull
J=1	for last card in a data set to be followed by another data set. Otherwise zero or blank
K=0	if 16 and 17 are in section II
1	if 16 and 17 are in section III

NFC Code

1 Maximum power condition (air vents closed)
2 Maximum power condition (air vents open)
3 "Free discharge" downstream from transition (pipe not full)
4 "Free discharge" (air vents closed, pipe full)
5 "Free discharge" (air vents open, pipe full)
6 Free discharge at gate

When the air vents are open, it is assumed that the net head=HEAD$-(H(28)-(0.640-C_e$ (geometry of Gate Opening))=HEAD$-(H(28)-E)$

$\therefore$ $E=0.640-C_e$ (geometry of Gate Opening)
Otherwise, $E=O$
B=Hg reading for section II
C=Hg reading for section III
D=Hg reading for section I or I′
E=(Defined above)
F=Elevation of the bottom of the top seal above the elevation of (28) when the flow is ventilated and $NGO \geq 10$
or
$NGO \leq 2$
Otherwise, $F=O$
G=Elevation of the top of the bottom seal above the invert when $NGO \geq 10$
or
$NGO \leq 2$
Otherwise $G=O$

PROGRAM FOR COMPUTING DOWNPULL ON A LARGE GATE FROM MODEL DATA

BUREAU OF RECLAMATION, DENVER COLORADO JUNE 1963

```
      DIMENSION A(8), HR(28), H(28)                                    2
      READ INPUT TAPE 5, 1, A                                          3
    1 FORMAT (8F8.3)                                                   4
      READ INPUT TAPE 5, 30, NEX                                       4A
   30 FORMAT (I4)                                                      4B
   32 WRITE OUTPUT TAPE 6, 31, NEX                                     4C
   31 FORMAT (1H1, 40X, 31H DOWNPULL STUDY, LIP EXTENSION , I2)        4D
    2 READ INPUT TAPE 5, 3, NGO, NFC, HEAD, J                          5
    3 FORMAT (2I4, F8.3, I4)                                           6
      READ INPUT TAPE 5,24, HR                                         7
   24 FORMAT (10F8.3)                                                  8
      READ INPUT TAPE 5, 4, B, C, D, E, F, G, K                        9
    4 FORMAT (6F8.3, I4)                                               10
      IF (K) 5,5,7                                                     11
    5 DO 6 I = 1, 20                                                   12
    6 H(I) = HR(I) + B * 13.58 - 0.79                                  13
      GO TO 11                                                         14
    7 DO 8 I = 1, 15                                                   15
    8 H(I) = HR(I) + B * 13.58 - 0.79                                  16
      DO 9 I = 18, 20                                                  17
    9 H(I) = HR(I) + B * 13.58 - 0.79                                  18
      DO 10 I = 16,17                                                  19
   10 H(I) = HR(I) + C * 13.58 - 0.79                                  20
   11 DO 12 I = 21, 24                                                 21
   12 H(I) = HR(I) + C * 13.58 - 0.79                                  22
      DO 13 I = 25, 27                                                 23
   13 H(I) = HR(I) + D * 13.58 - 0.79                                  24
      H(28) = HR(28) + C * 13.58 - 0.79                                25
      AVO = (H(25) + H(26) + H(27)) / 3.0                              26
      P1 = A(1) * AVO                                                  27
      S1 = C                                                           28
      DO 14 I = 4, 12                                                  29
   14 S1 = S1 + H(I)                                                   30
      P2 = A(2) * (H(1) + H(2) + H(3) + 2.0 * S1)                      31
      P3 = A(3) * (H(13)+ H(14) + H(15))                               32
      P4 = A(4) * (H(18)+ H(19) + H(20))                               33
      AV1 = 0.5 * (H(16) + H(17))                                      34
      P5 = A(5) * AV1                                                  35
      AV2 = 0.25 * (H(21) + H(22) + H(23) + H(24))                     36
      P6 = A(6) * AV2                                                  37
      P7 = A(7) * (AV1 + AV2)                                          38
      IF (NGO - 9) 50, 50, 16                                          39
   50 IF (NGO - 2) 16, 16, 15                                          39A
   15 P8 = 0.0                                                         40
      IF (NFC - 3) 26,25,25                                            40A
   25 P9 = A(6) * (AVO - AV2)                                          40B
      GO TO 17                                                         40C
   26 P9 = 0.0                                                         40D
      GO TO 17                                                         41
   16 P8 = A(8) * (AVO - H(28) - F)                                    42
      IF (NFC - 2) 26, 27, 27                                          42A

   27 P9 = A(6) * (H(28) + G - 0.64 - AV2)                             42B
   17 DPM =(P1 - (P2+P3+P4) / 3.0 - P5 - P6 - P7 + P8 + P9) * 0.433    43
      HN = HEAD - (H(28) - E)                                          45
      CF = DPM / (5.0418 * HN)                                         46
      HNP = HN * 7.80 / HEAD                                           46A
      IF (HNP - 8.10 - E) 29, 29, 28                                   46B
   28 HNP = 8.10 + E                                                   46C
   29 DPP = DPM * HNP * 42900.0 / HN                                   46D
      WRITE OUTPUT TAPE 6, 18, NGO, NFC, HNP                           47
  180FORMAT (1HO, 6X, 14H GATE OPENING , I2,  19H,   FLOW CONDITION    48
     1I2,  22H,   ADJUSTED NET HEAD=, F6.2)                            49
      WRITE OUTPUT TAPE 6, 19, H                                       50
  190FORMAT (12X, 7H H( 1)=, F7.3, 6F12.3 / 12X, 7H H( 8)=, F7.3,6F12.3 51
     1/ 12X, 7H H(15)= , F7.3, 6F12.3 / 12X, 7H H(22)= , F7.3, 6F12.3) 52
      WRITE OUTPUT TAPE 6, 20, DPM, DPP, CF                            53
  200FORMAT (7X,16H MODEL DOWNPULL=, F7.3, 23H,   PROTOTYPE DOWNPULL=, 54
     1 1PE11.3, 25H,   DOWNPULL COEFFICIENT=, 1PE11.3)                 55
      IF (J) 2, 2, 32                                                  61
      END(1,0,0,0,0,0,1,0,0,0,0,0,0,0,0)
```

DOWNPULL STUDY, LIP EXTENSION 3

GATE OPENING 2, FLOW CONDITION 1, ADJUSTED NET HEAD= 0.10

H(1)=	7.739	7.748	7.748	7.744	7.747	7.747	7.738
H(8)=	7.745	7.747	7.715	7.726	7.737	7.707	7.707
H(15)=	7.702	7.698	7.696	7.706	7.707	7.705	7.663
H(22)=	7.668	7.661	7.665	7.707	7.707	7.707	7.657

MODEL DOWNPULL= -0.070, PROTOTYPE DOWNPULL= -3.000E 03, DOWNPULL COEFFICIENT= -1.334E-01

GATE OPENING 3, FLOW CONDITION 1, ADJUSTED NET HEAD= 0.16

H(1)=	7.636	7.637	7.649	7.639	7.639	7.647	7.646
H(8)=	7.648	7.662	7.650	7.654	7.687	7.671	7.673
H(15)=	7.677	7.679	7.679	7.679	7.679	7.679	7.649
H(22)=	7.652	7.644	7.647	7.697	7.694	7.699	7.597

MODEL DOWNPULL= 0.200, PROTOTYPE DOWNPULL= 8.605E 03, DOWNPULL COEFFICIENT= 2.434E-01

GATE OPENING 5, FLOW CONDITION 1, ADJUSTED NET HEAD= 0.24

H(1)=	7.554	7.559	7.572	7.570	7.562	7.577	7.574
H(8)=	7.571	7.580	7.592	7.584	7.592	7.612	7.597
H(15)=	7.592	7.607	7.615	7.647	7.662	7.684	7.569
H(22)=	7.589	7.590	7.594	7.706	7.708	7.708	7.539

MODEL DOWNPULL= 0.626, PROTOTYPE DOWNPULL= 2.693E 04, DOWNPULL COEFFICIENT= 5.157E-01

GATE OPENING 7, FLOW CONDITION 1, ADJUSTED NET HEAD= 0.49

H(1)=	7.354	7.350	7.385	7.360	7.353	7.377	7.370
H(8)=	7.362	7.392	7.395	7.382	7.402	7.452	7.482
H(15)=	7.472	7.541	7.543	7.550	7.553	7.544	7.393
H(22)=	7.403	7.402	7.409	7.611	7.619	7.620	7.320

MODEL DOWNPULL= 1.047, PROTOTYPE DOWNPULL= 4.487E 04, DOWNPULL COEFFICIENT= 4.241E-01

GATE OPENING 9, FLOW CONDITION 1, ADJUSTED NET HEAD= 1.50

H(1)=	6.718	6.661	6.850	6.751	6.743	6.820	6.758
H(8)=	6.713	6.913	6.905	6.880	6.942	7.092	7.043
H(15)=	7.021	7.173	7.153	7.233	7.293	7.463	6.263
H(22)=	6.328	6.343	6.442	7.295	7.333	7.330	6.344

MODEL DOWNPULL= 2.214, PROTOTYPE DOWNPULL= 9.439E 04, DOWNPULL COEFFICIENT= 2.915E-01

GATE OPENING 10, FLOW CONDITION 1, ADJUSTED NET HEAD= 4.65

H(1)=	5.878	5.736	6.111	5.898	5.838	5.998	5.948
H(8)=	5.907	6.168	5.970	6.418	6.413	6.585	6.538
H(15)=	6.637	6.878	6.868	6.824	6.825	6.916	2.821
H(22)=	2.809	2.789	2.543	7.770	7.772	7.772	3.143

MODEL DOWNPULL= 11.097, PROTOTYPE DOWNPULL= 4.767E 05, DOWNPULL COEFFICIENT= 4.737E-01

GATE OPENING 11, FLOW CONDITION 1, ADJUSTED NET HEAD= 6.23

H(1)=	6.225	6.158	6.401	6.218	6.187	6.340	6.300
H(8)=	6.269	6.450	6.330	6.580	6.600	6.783	6.820
H(15)=	6.960	7.170	7.195	7.148	7.195	7.153	1.409
H(22)=	1.390	1.375	1.264	7.864	7.864	7.864	1.590

MODEL DOWNPULL= 11.204; PROTOTYPE DOWNPULL= 4.758E 05, DOWNPULL COEFFICIENT= 3.533E-01

GATE OPENING 12, FLOW CONDITION 1, ADJUSTED NET HEAD= 7.62

H(1)=	7.126	7.129	7.216	7.119	7.101	7.199	7.139
H(8)=	7.124	7.249	7.179	7.226	7.301	7.326	7.311
H(15)=	7.549	7.551	7.561	7.496	7.521	7.516	0.018

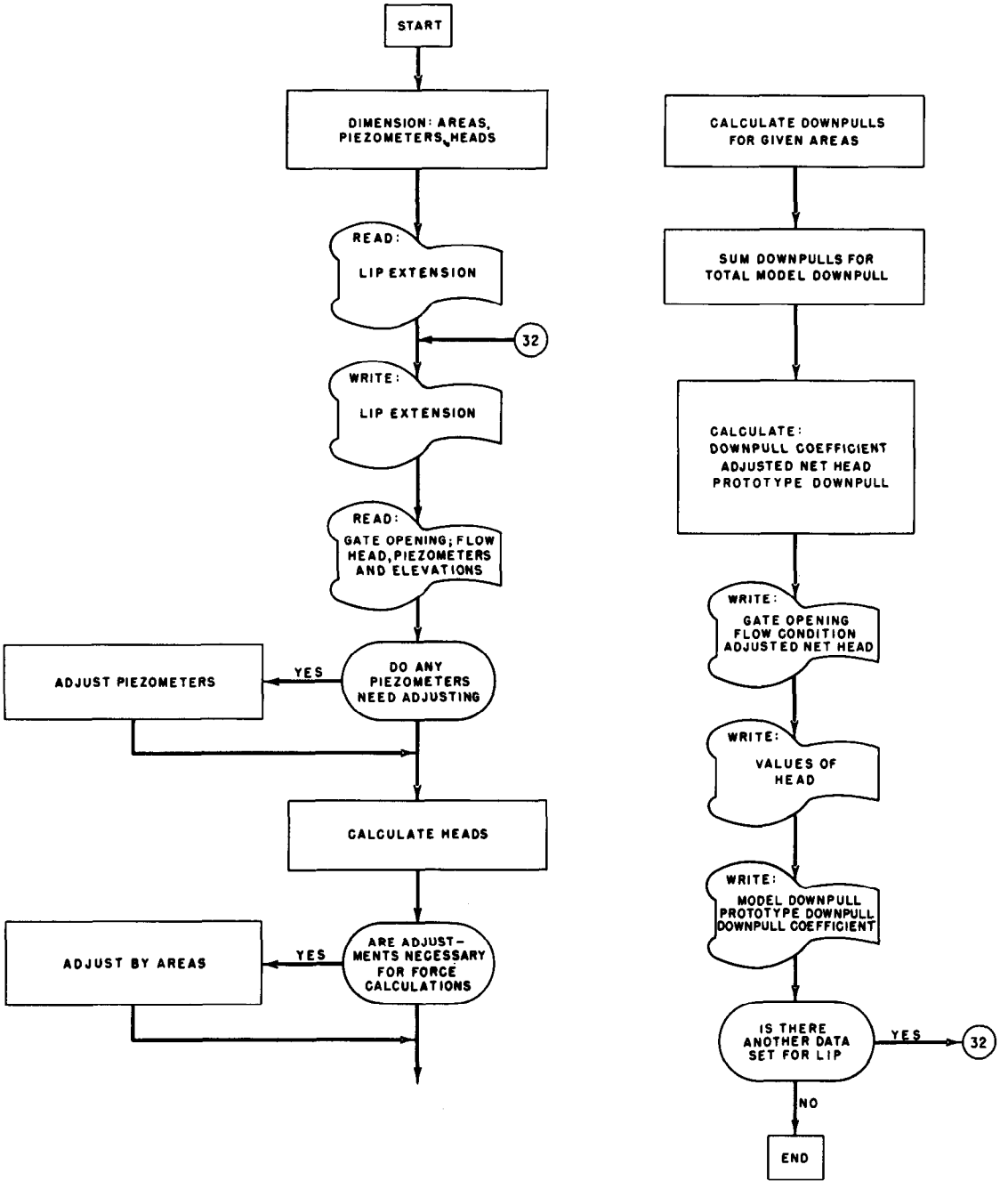

FLOW DIAGRAM

PROGRAM FOR COMPUTING DOWNPULL ON A LARGE GATE FROM MODEL DATA

ABSTRACT

General studies were made to determine design parameters for hydraulic downpull and uplift forces on downstream seal, roller-mounted gates located in entrance transitions of large conduits. Effects of various gate lip extensions, and recesses in the gate shaft, were investigated for one seal extension. Uplift forces great enough to prevent closure of gates under their own weight were found. Uplift forces were controlled by proper shaping of offsets and recesses in the face of the gate shaft or bonnet. A gate lip extension to leaf thickness ratio of 0.55 was selected as the optimum compromise between structural and hydraulic considerations. Pressures on the gate bottoms, and hence the downpull, were significantly affected by the gate slots and sidewalls. Effects of air admission were also determined. The data were applied to the 17.50- by 22.89-foot San Luis Outlet Works gates operating under a 273-foot head. Data are presented in both dimensional and nondimensional form.

Descriptors—*hydraulics/ *hydraulic downpull/ *air demand/ roller gates/ gate seals/ instrumentation/ hydraulic models/ intake gates/ cavitation.

Identifiers—hydraulic uplift/ lip extension/ seal extension/ bonnet recesses/ emergency closures.

☆U.S. GOVERNMENT PRINTING OFFICE: 1991—835-199